CHALMERS
UNIVERSITY OF TECHNOLOGY

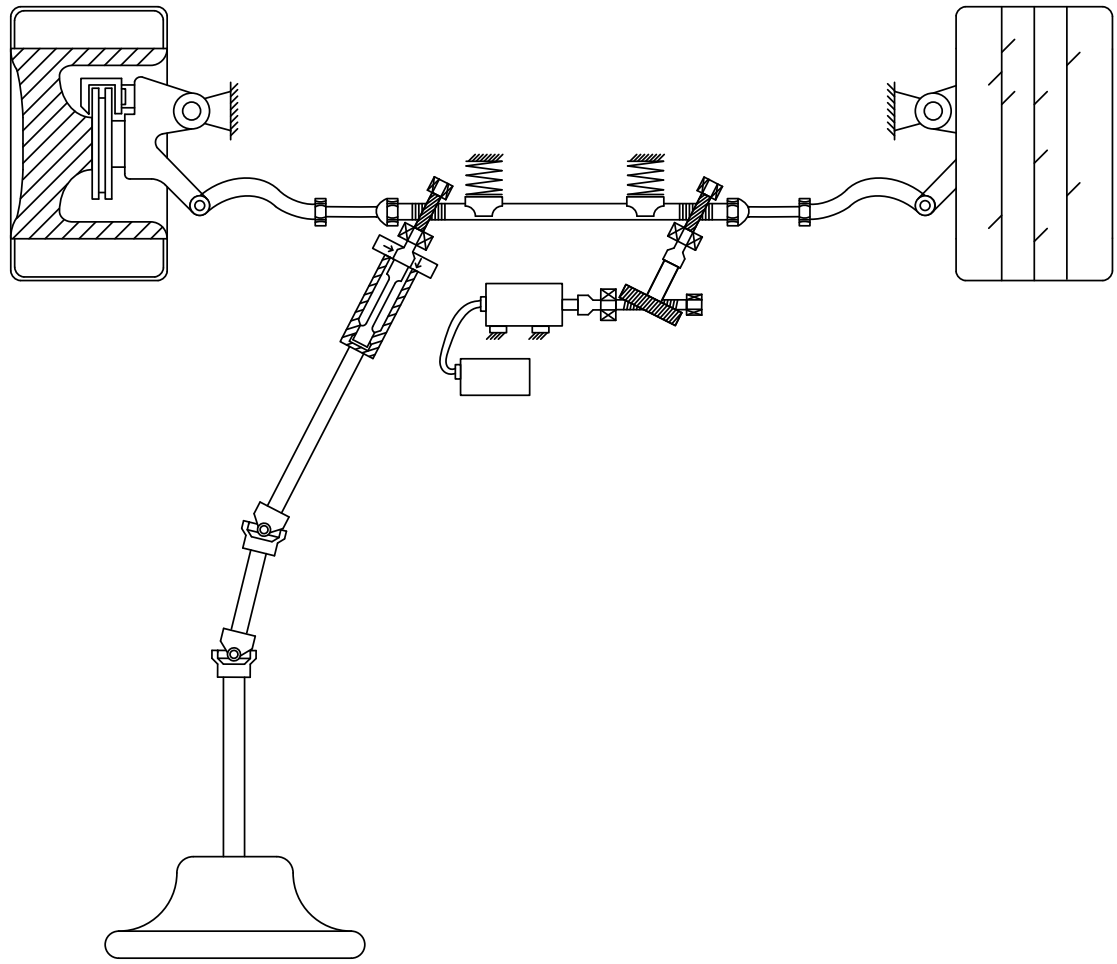

Functional Modelling and Simulation of an Electric Power Assisted Steering

Development of an advanced engineering tool

Master's thesis in Automotive Engineering

Albin Gröndahl

Department of Mechanics and Maritime Sciences
CHALMERS UNIVERSITY OF TECHNOLOGY
Gothenburg, Sweden 2018

MASTER'S THESIS IN AUTOMOTIVE ENGINEERING

Functional Modelling and Simulation of an Electric Power Assisted Steering

Development of an advanced engineering tool

Albin Gröndahl

Department of Mechanics and Maritime Sciences
Division of Vehicle Engineering and Autonomous Systems
Vehicle Dynamics group
CHALMERS UNIVERSITY OF TECHNOLOGY
Göteborg, Sweden 2018

Functional Modelling and Simulation of an Electric Power Assisted Steering
Development of an advanced engineering tool
Albin Gröndahl

Master's Thesis 2018:51
Department of Mechanics and Maritime Sciences
Division of Vehicle Engineering and Autonomous Systems
Vehicle Dynamics group
Chalmers University of Technology
SE-412 96 Göteborg
Sweden
Telephone: + 46 (0)31-772 1000

Examiner: Mathias Lidberg

Supervisor: Jan Hellberg
Ingemar Johansson
Mathias Lidberg

Cover:
Schematic image of the EPAS system layout. Figure has been entirely drawn by the author, Albin Gröndahl.

Department of Mechanics and Maritime Sciences
Göteborg, Sweden 2018-06-18

Functional Modelling and Simulation of an Electric Power Assisted Steering
Development of an advanced engineering tool
Master's thesis in Automotive Engineering
Albin Gröndahl
Department of Mechanics and Maritime Sciences
Division of Vehicle Engineering and Autonomous Systems
Vehicle Dynamics group
Chalmers University of Technology

Abstract

The automotive industry strives towards optimizing performance, efficiency and quality in every conceivable aspect. One area of development is the steering system that has for a long time been governed by the usage of the Hydraulic Power Assisted Steering system (HPAS) throughout the automotive industry. As requirements demand higher efficiency, the need for a more flexible system increases. The alternative of Electric Power Assisted Steering systems (EPAS) provides the desired flexibility but also introduce issues with system inertia and vehicle stability. The demand for virtual development processes gives rise to a need for functional models of the EPAS system. This thesis includes developing a functional EPAS-model as well as investigating the fundamental effects of the EPAS system nature with regards to geometry and controller functionality.

Key words: Electric Power Assisted Steering, Electric Power Steering, Steering, Steering Control, Steering Modelling, Steering Feel, Steering Tuning, Vehicle Tuning, Vehicle Dynamics, Automotive CAE, Modelling and Simulation, Model Follower Control Strategy.

Contents

Preface

This project came to me while discussing possible master theses with supervisor Ingemar Johansson. The opportunity suddenly arouse and my efforts in finding a thesis project were victorious. For half a year, I was involved in creating the scope and objective with the project.

I have been getting to know many people at CEVT, the home of the project, since the work started. It has been inspiring to see other people succeeding but also struggling. Conducting a master thesis project alone has been tough, I have learned, but thankfully, there are many people around me that has been the support needed throughout the hard work.

Most importantly, I have learnt a tremendous number of new things while conducting this research and development venture. I also hope that the outcomes of the project can become the foundation for something else, if it is another thesis project or maybe the key for someone who just seems to not be able to crack that little piece of the puzzle. During the project, I have been there many times. Suddenly, however, the quest is finished and the next day, there are new adventures.

Göteborg 2018-06-18

Albin Gröndahl

Notations

AD	Active damping	[N]	Variable
c_{TB}	Torsion bar rotational stiffness	[Nm/rad]	Parameter
d_{TB}	Torsion bar rotational damping	[Nms/rad]	Parameter
$F_{damp,M}$	Motor damping	[Ns/m]	Parameter
$F_{damp,R}$	Rack damping	[Ns/m]	Parameter
$F_{damp,SW}$	Damping force steering wheel	[Ns/rad]	Variable
$\mathrm{F_{ESF}}$	Elastic spring friction force	[N]	Variable
$\mathrm{F_{ESF,d}}$	Elastic spring friction damping force	[N]	Variable
$\mathrm{F_{ESF,s}}$	Elastic spring friction spring force	[N]	Variable
$F_{fric,R}$	Rack friction	[N]	Variable
$F_{fric,SW}$	Steering wheel friction	[Nm]	Variable
F_K	Rack force from tie rods	[N]	Variable
$F_{limit,R}$	Friction force limit rack	[N]	Parameter
$F_{limit,SW}$	Friction force limit steering wheel	[N]	Parameter
F_M	Rack force from servo motor	[N]	Variable
$F_{M,hysteresis}$	Required force hysteresis	[N]	Variable
$F_{M,linear}$	Required force linear servo	[N]	Variable
$F_{M,quadratic}$	Required force quadratic servo	[N]	Variable
$F_{M,req,BSA}$	Required force basic steer assist	[N]	Variable
$F_{M,req,FB}$	Required force feedback controller	[N]	Variable
$F_{M,req,FF}$	Required force feedforward controller	[N]	Variable
F_{TB}	Rack force from sensor pinion	[N]	Variable
$F_{tyre,lat}$	Tyre lateral force	[N]	Variable
I_M	Servo motor current	[A]	Variable
J_M	Servo motor inertia	[kgm^2]	Parameter
J_{SW}	Steering wheel inertia	[kgm^2]	Parameter
$k_{1,hyst}$	Hysteresis coefficient	[-]	Parameter
$k_{1,quadratic}$	Quadratic servo coefficient	[-]	Parameter
$k_{2,hyst}$	Hysteresis coefficient	[-]	Parameter
$k_{2,quadratic}$	Quadratic servo coefficient	[-]	Parameter
$k_{3,hyst}$	Hysteresis coefficient	[-]	Parameter
$k_{4,hyst}$	Hysteresis coefficient	[-]	Parameter
$k_{arbitration}$	Arbitration variable	[-]	Variable
$k_{d,limit,R}$	Damping limit coefficient rack	[Ns/m]	Parameter
$k_{d,limit,SW}$	Damping limit coefficient steering wheel	[Ns/m]	Parameter
$k_{d,stiffness,R}$	Damping stiffness coefficient rack	[-]	Parameter
$k_{d,stiffness,SW}$	Damping stiffness coefficient steering wheel	[-]	Parameter
K_E	Speed coefficient	[Vs/rad]	Parameter
$k_{ESF,R}$	Friction stiffness coefficient rack	[Nm]	Parameter
$k_{ESF,SW}$	Friction stiffness coefficient steering wheel	[Nm]	Parameter
$k_{lin,servo}$	Linear servo coefficient	[-]	Parameter
$k_{main,damp1}$	Damping coefficient	[-]	Parameter
$k_{main,damp2}$	Damping coefficient	[-]	Parameter
$k_{main,damp3}$	Damping coefficient	[-]	Parameter
$k_{MTB,damp}$	Damping coefficient	[-]	Parameter
K_T	Torque coefficient	[Nm/A]	Parameter
$k_{TBR,damp}$	Damping coefficient	[-]	Parameter

L_M	Servo motor inductance	[mH]	Parameter
$Main_{damp}$	Main damping	[-]	Variable
m_R	Rack mass	[kg]	Parameter
$m_{R,des}$	Desired rack mas	[kg]	Parameter
M_{TB}	Torsion bar torque	[Nm]	Variable
$M_{TB,damp}$	Torsion bar torque damping	[-]	Variable
nst	Steering ratio	[-]	Parameter
r_K	Steering arm length	[m]	Parameter
r_M	Effective radius motor pinion	[m]	Parameter
R_M	Servo motor resistance	[Ohm]	Parameter
r_{SW}	Radius steering column friction lever	[m]	Parameter
r_{TB}	Effective radius sensor pinion	[m]	Parameter
SWT	Steering wheel torque	[Nm]	Variable
TBR_{damp}	Torsion bar torque rate damping	[-]	Variable
T_M	Servo motor torque	[Nm]	Variable
t_{caster}	Caster/mechanical trail	[m]	Variable
t_{tyre}	Pneumatic trail	[m]	Variable
V_M	Servo motor control voltage	[V]	Variable
V_{veh}	Vehicle longitudinal velocity	[m/s]	Variable
y_R	Rack lateral displacement	[m]	Variable
$y_{R,error}$	Rack lateral displacement error	[m]	Variable
$y_{R,ref}$	Reference rack lateral displacement	[m]	Variable
τ_{TBR}	Torsion bar deformation	[rad]	Variable
ϕ_{SW}	Steering wheel angle	[rad]	Variable
ω_{SW}	Steering wheel rotational velocity	[rad/s]	Variable

1 Introduction

In the modern history of humanity, transportation has been a key area of both problems and development. As the need for higher flexibility in the location of certain people or equipment increases, the means of transportation should evolve as well. The industrial revolution is a perfect example as the introduction of the railway, which was a central part of the 19th century technical developments, handled the issue of transportation. Large portions of the technical advances in recent years has been on transportation and its supportive functions. The automotive industry is no exception and in the last century, cars has been developed from a horse carriage state of similarity to the technical wonders they are today. In this progress there are many vehicle attributes that has greatly improved, such as safety, quality, comfort and performance. Multiple attributes are opposing each other but thorough research and development has made it possible to increase these attributes significantly, without a too big compromise. Vehicle dynamics, and specifically handling, together with comfort is such an example. The handling ability of cars has been improved substantially in the last decades combined with the increased comfort.

A vital aspect of handling, as well as feedback to the driver, is the steering system. To achieve a higher comfort while driving cars, the power assisted steering system was introduced. This meant that the driver no longer had to provide all the force needed in the steering system for controlling the vehicle during for instance parking, on-centre driving or during highly dynamic driving conditions, which all have entirely different performance requirements. The suspension and every mechanical part of the steering system could then be developed to increase the system robustness regarding durability and feedback quality instead of minimizing rack forces. The standard solution for providing the steer assist force, was for a long time the Hydraulic Power Assisted Steering (HPAS) and automotive companies refined the system characteristics to near perfection. However, the flexibility in the HPAS system over time, as well as efficiency, was low. The event that triggered the switch to more complex systems was partly the need for extra steering functions on vehicle level but also due to easier installation without the hydraulic system installation.

An example of a complex steering system offering a greater amount of flexibility is the Electric Power Assisted Steering system (EPAS). With the EPAS comes the ability to switch the assist on or off during driving and having a dynamic tuning and motor mapping. The HPAS systems had to be tuned by design of the hydraulic valves but the EPAS can be controlled entirely through software (Wallnäs, 2015). However, due to the high gear ratio on the motor, the inertia is increased significantly (Ljungberg, 2014). With this inertia comes issues that has not been dealt with before. The inertia acts as a low pass filter to the force feedback for the driver from the road (Chugh, Chen, Klomp, Ran, & Lidberg, 2017). The controller of the EPAS system must thereby deal with the compensation of this inertia and the multiple side effects it gives.

The control strategy of the EPAS has been developing since the system first appeared. The steering feel of these systems has been given criticism by motor journalists and automotive companies has put a lot of effort into giving the system a better steering feel (Smith, 2018) (Fernie, 2018). This development has given a set of different control strategies redefining how to think about the concept of steering feel. These strategies will be handled to some extent in the thesis.

1.1 Problem motivating the project

To analyse, understand and set development targets for attributes in vehicle development projects regarding handling and steering, there is a great benefit to have functional simulation models. Depending on what phase the project is in, the complexity of the model should be in the suitable magnitude. In early phase development, there is a need for a model that is as simple as possible so that the input data are reasonably easy to retrieve but as detailed as necessary to predict the basic performance and system dynamics. Later, in the development process, the complexity of the models should increase to better portray the full solution.

1.2 Envisioned solution

The envisioned solution is an EPAS functional simulation model including the system mechanics and servo assist functions giving the basic dynamic response. The model should be usable as a tool to analyse, understand and set development targets as well as support requirements setting and verification. The tool should not focus on defining or capturing individual component behaviour but might include simplistic component design for added robustness and precision.

1.3 Objective

Develop a simulation model using e.g. MATLAB, Simulink, VI-CarRealTime and Adams/Car as required, of an EPAS system that can be used in simulation to gain knowledge in the area of research and development. This means that the system as a whole should be studied regarding system elasticity, hysteresis (i.e. dynamic friction effects over time) and inertia effects including electric motor dynamics and servo assist but not component design parameters such as joint friction. The system to be modelled is a dual pinion system. The model is to be simulated in conditions similar to:

- On-centre and straight ahead driving.
- Vehicle stability during external disturbances.
- Vehicle dynamics standardized testing scenarios.
- Highly dynamic manoeuvres.

1.4 Deliverables

- A model of the EPAS system for easy simulations.
- The model in a co-simulation together with for instance VI-CarRealTime.
- Simulation results using the developed model in scenarios as specified in Paragraph 1.4.

1.5 Limitations

- No subjective analysis of the steering feel, only objective.
- No development of a fully working controller.
- No development of specific components.
- Use existing front and rear suspension geometries.

2 Background

2.1 Steering system architecture

In the EPAS system, there is an electric motor providing the extra force that is required to assist the driver, instead of the hydraulic servo assist which is the type of assist in the HPAS systems (Harrer & Pfeffer, 2017). In this thesis, a dual pinion system, shown in Fig 1, has been modelled and evaluated. On the rack, there are two pinions for rack actuation. These are the sensor pinion, named so because of the location of the torsion bar, and the motor pinion. The steering wheel and column are attached to the torsion bar and then connected to the rack at the sensor pinion, delivering the torque provided by the driver converted as a force on the rack. This torque is what is measured in the torsion bar. The motor is connected to the motor pinion through a worm gear, increasing the gear ratio. This gear ratio is crucial for delivering enough force from the motor, since the rack needs thousands of Newton of force when driving in certain conditions. However, the rack does not need to move quickly, justifying the use of a higher gear ratio. Therefore, the motor torque is increased through gearing, at the expense of higher required motor rotational speeds. Several relevant components can be found in the above description of the EPAS system. These are, together with some other components and important terms, described in the following sections.

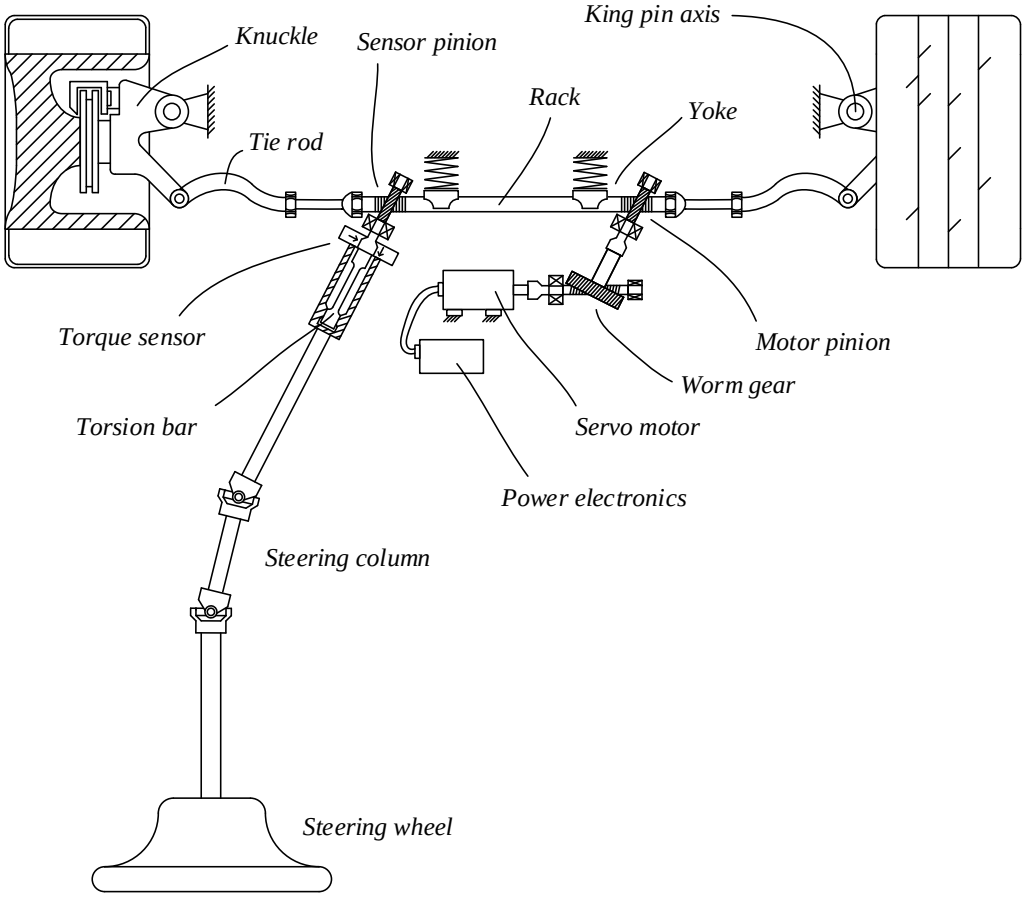

Fig 1. A schematic image of the dual pinion EPAS system.

2.1.1 Rack

The rack is the component subject to all forces in the system, acting as the central piece of the steering. All interactions in the dual pinion system must act through the rack, as none of the steering column, the servo motor or the wheel knuckles connects directly. The rack can therefore supply crucial information about the steering system states for the system controller. As the rack moves, the wheels are steered by the tie rods moving with the rack. This further stress the importance of the states of the rack.

The rack is suspended by the two pinions, shown in Fig 1, and their corresponding yokes. The yokes allow the rack to slide while keeping it pressed against the pinions. The yoke is a source of friction and the correct amount of preloading in the spring behind the yoke is crucial. Too little preloading gives the rack too high a play and might harm the interaction with the pinion. On the other hand, a too tight yoke will cause the rack to be fixated by excessive friction. In Fig 2, the rack can be seen in axial view with a yoke and pinion supporting it from either side.

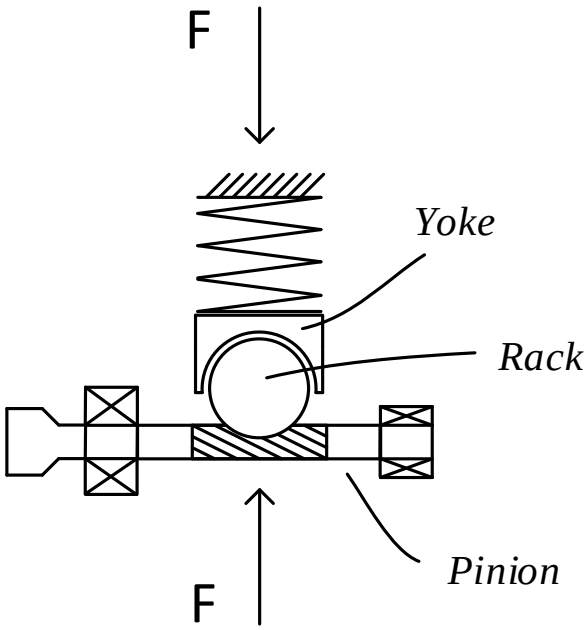

Fig 2. A cross section of the steering rack suspended by the yoke and pinion.

2.1.2 Servo motor

The servo motor can be of either direct current or alternating current type. A key parameter of the motor is the rotational inertia. Due to the high motor transmission gear ratio, the torque required by the system from the motor is low and thereby the motor size, and ultimately the inertia, can be kept low. However, the gear ratio amplifies the inertia acting on the rack by a quadratic expression. When accelerating the rack, for instance by forces from the tyres coming through the tie rods, the motor must accelerate at a higher rate than the rack, given by the gear ratio. This is equivalent to demanding a higher amount of acceleration in the motor that in turn gives a higher impact of the inertia or a higher fictive inertial force. The gear ratio also increases the impact of this force on the rack, effectively making the motor stronger in every situation, giving the quadratic expression describing the inertia relationship. The equivalent rack mass is

given in Equation 1, giving a result of about 1500 kg, mainly originating from the parenthesis of the motor inertia divided by the effective motor radius squared. The real rack mass is small in comparison, weighing in at just a couple of kilograms. This gives a low-pass filter function in the mechanical parts of the EPAS system, meaning that high frequent information in the shape of forces going through the rack are filtered out. This diminishes certain areas of the road feel for the driver, regarding quick changes in the grip level or from disturbances. Since all forces are passing the rack, due to it being the central system component, this effect is significant and cannot be compensated for mechanically while utilizing the electric motor solution.

$$m_{R,eqv} = m_R + \left(\frac{J_M}{r_M^2}\right) \tag{1}$$

The vehicle eigenfrequency is normally about 1-1.5 Hz and the conventional steering systems, such as HPAS, had a significantly higher eigenfrequency based on the system inertia or mass and the stiffness of the tyres as well as suspension geometry. With the introduction of the EPAS, however, the inertia of the motor on the rack affects the eigenfrequency so that it ends up closely to the vehicle eigenfrequency, losing the steering system ability to self-align quickly, causing the vehicle to turn unstable at certain velocities without controller or driver interventions (Sakai, 2014). This aspect has been a key area of research throughout the project.

2.1.3 Torsion bar

The main sensor in the system is the torsion bar (Fig 3). It measures roughly the torque provided by the driver relative to the rack. It is important to understand that this torque is the torque between the steering column and the sensor pinion. Newton´s 3rd law should be considered as there is an equal and opposite force from the opposing side. This means that the sensed torque may in fact be the input from the steering system to the driver and not necessarily the driver input. Another aspect to include in the torsion bar characteristics is that a part of the torque might be lost between the steering wheel and the torsion bar due to friction and other losses, such as inertial forces interference.

An issue with the torsion bar is its high compliance. The torsion bar measures the torque by measuring the angular twist from top to bottom of the bar. The stiffness is known, and can be calibrated, which in turn gives the torque (Van Ende, Kallmeyer, Nippold, Henze, & Kucukay, 2016). To have a high enough angular deformation to give a measurement with sufficient precision, the torsion bar stiffness must be low. For increasing the steering feel, a stiffer steering is normally wanted and in some cases, the torsion bar is limiting in this aspect (Harrer & Pfeffer, 2017). Research is ongoing in the subject of new torque sensor types and there are some new technologies being tested.

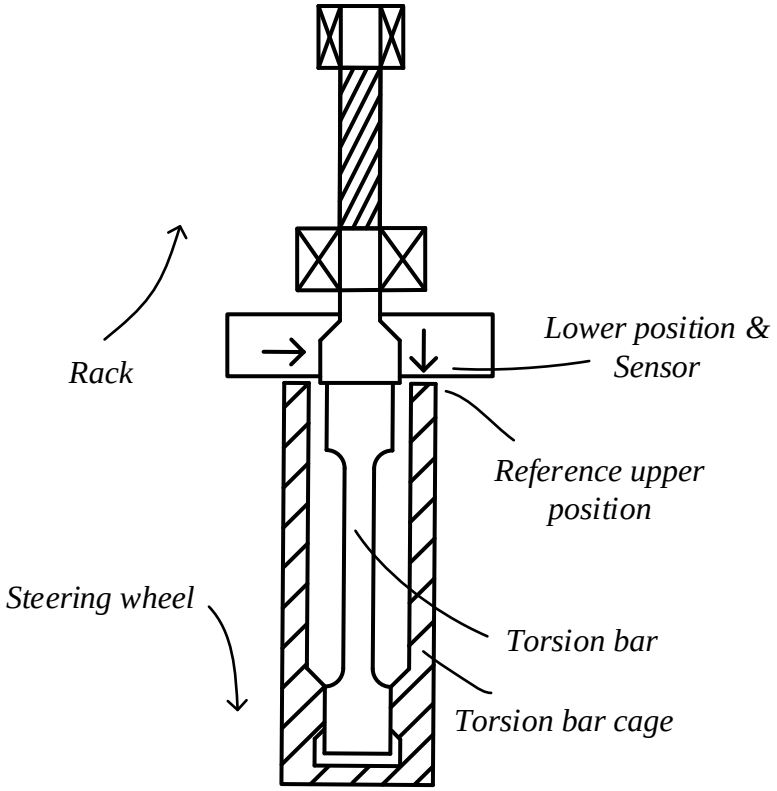

Fig 3. The torsion bar in a schematic image.

2.2 Mechanical analysis

There are four main types of forces acting on the rack in the dual pinion EPAS system at five locations, assuming that friction acts at a certain spot. These is shown in Fig 4. Through this paragraph, the forces will be explained more closely.

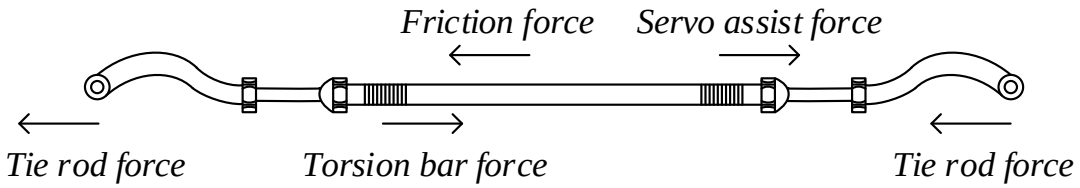

Fig 4. The rack with the main forces drawn.

Firstly, the force resulting from the torsion bar torque or the torque in the sensor pinion will be discussed. This torque comes from the steering column and the resultant of the torques on it. This means that it is not only the driver torque that goes into the torsion bar but the sum of the driver torque, the torque provided by the friction on the steering column as well as the inertial forces (Fig 5). If the driver releases the steering wheel, the friction force and the inertia in the column gives a potentially non-zero torque in the torsion bar, depending on its states.

Fig 5. Illustration of the torques acting on the inertia of the steering column.

The second force on the rack is the force resulting from the torque in the motor pinion. This torque is more complicated than the steering column torque due to the more complex components in the motor transmission, shown in Fig 6, as well as the motor controller. There is another worm gear introducing more friction and the gear ratio in itself complicates the dynamics further. The motor inertia is multiplied with the gear ratio squared and then acting on the rack. The torque from the motor is governed by the electrical circuit, meaning that the motor torque modelling must cover the electrical dynamics.

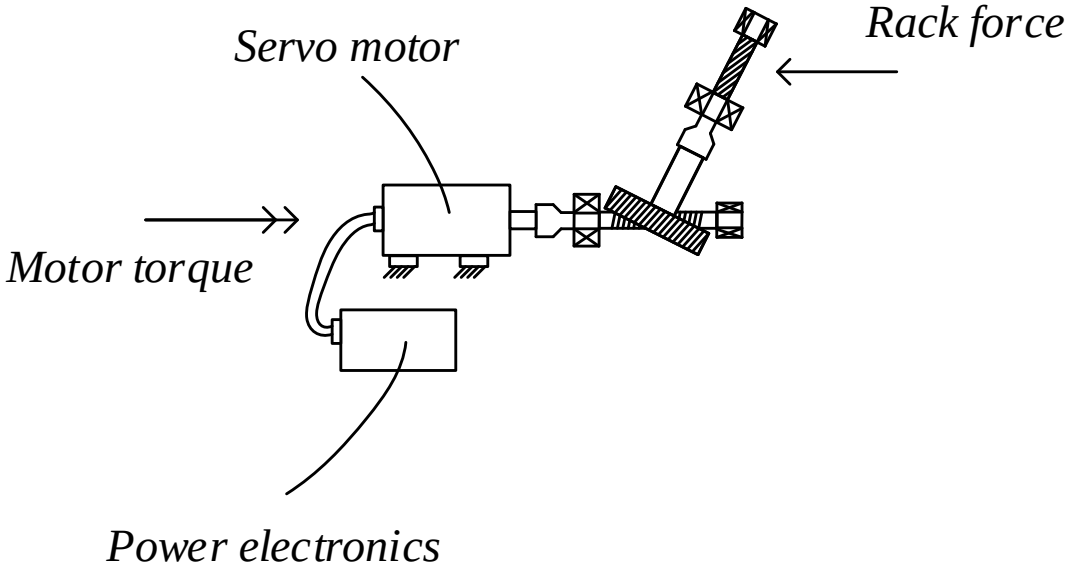

Fig 6. Torques and forces on the servo motor transmission.

The force given by the interaction between the vehicle and the road is the third force explained here (Fig 7). When cornering, the tyre builds up slip which in turn produces a force acting on the tyre that accelerates the vehicle in the corresponding direction. The wheels are mounted to the hubs or knuckles in a way that constrains the wheel steering motion, giving a resisting torque around the King Pin Axis (KPA). The offset from the KPA is given by the sum of the fixed caster trail and the dynamic pneumatic trail. As the lateral force changes, the pneumatic trail does as well. This combined offset is the lever for determining the force taken up by the tie rod which gives the resisting torque around the KPA. The tie rod force goes into the rack and acts as an opposite force compared to the sensor pinion force and the motor pinion force. The torque on the wheel is thereby called the aligning torque. Depending on the location of the rack and thereby the tie rods, this rack force from the knuckles has the same or the opposite

direction as the tyre lateral force. Due to the inherent inertia issue with the EPAS, the tie rod force is filtered out to some extent. This means that it does not propagate in the desired manner to the sensor pinion and to the driver. The rudimentary steering feel in the EPAS system is thereby insufficient due to the mechanical layout.

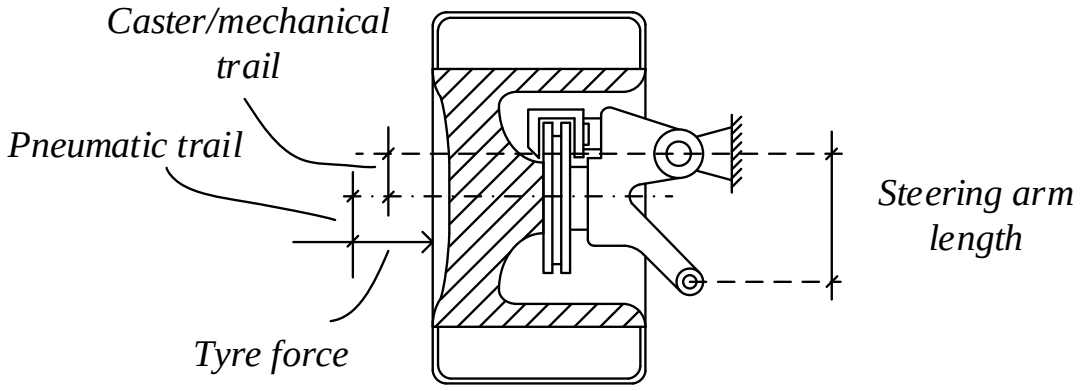

Fig 7. A top view of the suspension in an illustrative manner, showing levers and acting points of forces.

As mentioned for the steering column, the friction forces are a vital aspect of the essential dynamics of the EPAS system (Van Ende, Kucukay, Henze, Kallmeyer, & Hoffmann, 2015). The yoke operation on the rack produces friction forces that are both wanted and unwanted. They give a stability to the system but they are often considered among behaviours or phenomena that should be counteracted for. The friction forces act in the opposite direction of the movement of the component in question. It depends both on how far the component has moved, since the force build-up is not instantaneous, as well as the velocity of the frictional surface. A significant increase in friction force due to velocity requires high velocities between surfaces which is normally not the case for any of the EPAS components.

2.3 Steering system controller

With the addition of the electric motor in the EPAS system, the ability to actively control the servo force is given. This ability is necessary to overcome some issues that are inherent in the system. However, the issues are also given by the motor installation and therefore, the cause of the problems also enable the solution. That is, the inertia in the motor is the major source of these issues but the motor can also be used to compensate for it, as well as for other characteristics, by altering the servo force provided, dynamically. To achieve a significant level of system function, extensive control strategies are required. The steering and road feel is an important aspect of the steering system as it is a central part of the feedback to the driver. Without a reasonable steering and road feel, the driver might not be able to drive the car in a safe manor. To look further into the subject, steering feel and road feel should be defined.

2.3.1 Steering feel

The steering feel is the relationship between the steering wheel torque (SWT) and the steering wheel angle (SWA) (Gruner, Gaedke, Hsu, & Harrer). Other relationships are classified differently, such as SWT to lateral acceleration which can be called road feel. As the driver increases the SWA, the response or feedback torque, the SWT, should

change in some way. The way the driver increases the SWA is by supplying a larger torque than the current feedback torque, meaning that the feedback torque cannot be too large or increase too rapidly. The torque feedback is normally separated into segments of the SWA range. The first part closest to the centre or zero SWA defines the torque build up. Much of the perceived steering characteristics comes from the shape of this area of feedback (Gruner, Gaedke, Hsu, & Harrer). Outside this central part of the steering, the target is mainly to give the driver an idea of how hard the cornering is and the level of available grip.

2.3.2 Road feel

A necessary ability of the steering system is to convey information from the road through the steering, such as irregularities and grip level. The road feel is thereby normally given by the relationship between SWT and lateral acceleration. The lateral acceleration and lateral tyre force are closely coupled, permitting the driver to estimate the road conditions and utilisation of it by the feel in the steering wheel as well as the lateral acceleration felt in the body. As the vehicle approaches the handling limit during cornering, the feedback torque should drop, as it is a sign of degressive lateral force into the front tyre. The road feel is somewhat of a compromise in comparison to the steering feel as the initial yaw rate is high with high road feel but a high initial yaw rate impairs the torque build-up for the steering feel, creating a complex compromise for steering feel development (Gruner, Gaedke, Hsu, & Harrer).

2.3.3 Implementation

To achieve the desired steering and road feel, automotive companies and researchers are conducting research on the area of how to produce the best reference generator (Chugh, Chen, Klomp, Ran, & Lidberg, 2017) (Uselmann, Kruger, Bittner, & Rivera, 2015). There are two ways to create a reference since the mechanical system has two variables available to the driver. They are the SWA and the SWT. To build a reference, one of these should be measured and the other should be the feedback, simply put. This means that for the controller to operate, it needs an input, whether it is the SWT or the SWA. Based on this input, the controller can then alter the other variable. In other words, the controller is a function with either the SWT or the SWA as input and the other one as an output to the driver.

One reference generator solution is to set up a virtual rack with a low mass and estimating all forces on the real rack and applying them to the virtual rack. The states of the virtual rack are then followed by the real rack by minimizing the state errors, called model following (Abe, 2015). This can be used for numerous implementations in the automotive industry (Raksincharoensak, Lertsilpachalern, Lidberg, & Henze, 2017). The reference generator type of this method is the steering wheel torque reference generator. It measures the steering wheel torque, and the rest of the rack inputs, and decides on the steering wheel angle response of the system. This action also gives an inertia compensating effect as the system works as a system with lower inertia. This increases the system responsiveness as desired, but can also induce instability in the system (Chugh, Chen, Klomp, Ran, & Lidberg, 2017). The controller can be supplemented with an active damping function to increase stability while maintaining the responsiveness of the system, thus creating a desired solution.

3 Method

Herein are the descriptions of methods of modelling and development of the model and control strategies as well as simulation methods. The target of the section is to give the reader increased knowledge about the work process and information on how to model the given type of mechanical system.

3.1 Modelling

The modelling of the system has been conducted in Simulink. When using Simulink there are certain things to address that in other software are already taken care of. Keeping track of the unit for each signal while building the model is such a task. The unit does not need specification but for modelling, there is no check to run for confirming that the signal units are compatible. If multiplying a force with a distance, effectively a lever, the signal then becomes a torque. For Simulink however, the signal just becomes a new value. There is also no separation between physical quantities or signal values, whether it is an electrical signal in a cable or for instance a force. Simulink is modelled with causality meaning that there is a clear flow of data through model components giving Ordinary Differential Equations (ODEs) instead of having for instance a physical interface. Modelica is a language that handles this type of interface and can model mechanics as well as algorithms and mechatronic systems, being acausal. It does this through implementation of Differential Algebraic Equations (DAE). Since Simulink is not acausal as Modelica is, the modelling method needs to account for this difference (Jacobson, 2016).

Modelling the mechanical components require some decisions on which signals to use and in what order to compute results. For instance, looking at the torsion bar that is an element that is governed by its deformation and force response. In reality, the interface on both sides have two interface variables, the force and the position. Both are inputs and both are outputs since the force is clearly connected to the deformation and vice versa. However, it is the increase in force that results in a larger deformation, rendering the force as a suitable choice of input variable in simulations. On the other hand, the component connected to the torsion bar is a mass whose movement is based on equations of motion or the sum of forces resulting in an acceleration, that is. This means that the force in the torsion bar interface should preferably be given to the connected mass as a response variable, not as the interface input to the torsion bar. This aids the modelling conformity of modelling movement of masses with equations of motion.

The result of this reasoning is that there are two ways of modelling the torsion bar, where one is preferred due to the reasons in the above paragraph. The first way is to supply the forces acting on the component, in this case the torque on each side of the bar, and then calculating the resulting deformation based on component stiffness and similar parameters. The other option is to supply the positions on each side of the bar, i.e. both angles of the ends of the bar, effectively giving the deformation, which is the difference in those angles. Then the current torque through the torsion bar can be calculated based on component stiffness and possibly damping. Comparing to reality, the second option emulates the scenario better, and it was also chosen above. The reason for that is that the difference between both angles can be measured precisely (that is the measurement actually taking place in the torsion bar). Using signals that are present in the real world is advantageous. The torque measured in the torsion bar is calculated

using the known component parameters together with the deformation measured. Modelling the component in this way is at least as good as the first alternative, giving the ability to induce sensor modelling as well. Even though the mechanics are reversible, the system functions are not. Choosing the corresponding way might not give an advantage directly but intuitively, it minimizes the diversity between modelling and reality. As a result, the positions are the input for the torsion bar and the forces are the responses. This is supported by both reasons in this and the previous paragraph.

The equations of motion are the fundamental equations governing the system states. The sum of forces acting on a mass or inertia gives the acceleration of that degree of freedom. The acceleration is integrated, giving the velocity and integrated again for position. These positions are normally used for calculating the response force coming from for instance the torsion bar or the tyres. The driver gives a torque input to the steering wheel depending on desired steering wheel angle giving the response force. Similarly, the lateral tyre force is mostly dependent on steering wheel angle, together with the vehicle state, giving the force response for rack displacement. The main contributor to determining friction forces is also the position. In summary, the positions in the system gives the response forces. The velocities however, gives rise to damping forces in the same way as inertia is coupled to accelerations. In general, the states (accelerations, velocities and positions) are used to determine response forces of different kinds. These forces are fed into the equations of motion to calculate the new acceleration which then gives the system states in the next step. Simulink solves these equations and handles the solver settings if that is desirable.

Since the torsion bar is considered significantly more compliant than the rest of the components, the modelling of the system in this thesis has been conducted using a 2 Degree of Freedom (2-DOF) approach. This means that the Steering Wheel Angle (SWA) and the wheel steering angle (δ), with translation using the steering ratio relationship (n_{st}), cannot be considered equivalent since the torsion bar deformation introduces compliance understeer. This means that the driver needs to steer more with the steering wheel, divided with the steering ratio, to achieve a certain wheel steering angle. The more compliance in the torsion bar, the more the driver must compensate for the deflection of it. These two, the SWA and δ, represent the two DOFs in the system. This means that the rack and motor movement as well as the lower mount of the torsion bar is connected to δ with ratios and the steering column together with the upper mount of the torsion bar coincides with SWA. This approach is a delimitation in complexity, as every part has a compliance in the real system, but it captures the system dynamics and general behaviour. This modelling shows the inherent issues with the EPAS system and its inertia as well as the performance of the control strategy solutions.

The system input in vehicle dynamics simulations is normally steering wheel angle (SWA) since it clearly defines the movement of the vehicle, but to analyse the steering system dynamics in a representative way, the input must be the steering wheel torque (SWT) since that is the real input. A force is the only way to affect the mechanical system, it cannot be actuated by a displacement. Since the model implements equations of motion based on forces and thereby emulates these characteristics, this applies to the model as well. For modelling purposes, model consistency as well as system representation, the SWT is used as input. The intended steering wheel angle is thereby controlled by a controller giving the SWT to minimize the error in the current SWA to the reference SWA.

3.2 Simulation

Simulations were initially performed for development of the model. The results were used for troubleshooting and debugging of the growing model. Without the ability to continuously simulate the model, errors and improper modelling could not have been detected efficiently. For verifying the system, another simulation model was used as a benchmark, meaning that verification of the model relied on differences in simulations of itself and the more complex model. Long before the model produced results of interest, simulations were used to extend and develop it. Developing a model thus means running the current state of it to try and improve on it. Not until the model was finished, useful results were produced for the first time. The production of data is often regarded as the purpose of the simulations of the model. However, the majority of simulations has throughout this project consisted of the development and troubleshooting simulations.

3.2.1 Simulation environment

To acquire realistic results from the simulations on the steering system, the vehicle used together with it was implemented in VI-CarRealTime (CRT). CRT uses information in the form of lookup tables or similar that can be either created directly in the tool or from data from other software such as Adams/Car. Since the EPAS was modelled in Simulink, an implementation had to be found or developed. VI Grade, the company developing CRT, had such an implementation method. They provided a Simulink block that uses data files created in CRT containing vehicle and environment information as well as driver data for the current driving scenario (Fig 8). The inputs and outputs in this block could be customized to suit the current simulation. The EPAS model was put in the same Simulink model and the appropriate connectors were connected. After the simulation completion, a results file according to the CRT standard was created. The data set in the working directory was available from MATLAB as well, providing a co-simulation interface with a desired level of accessibility.

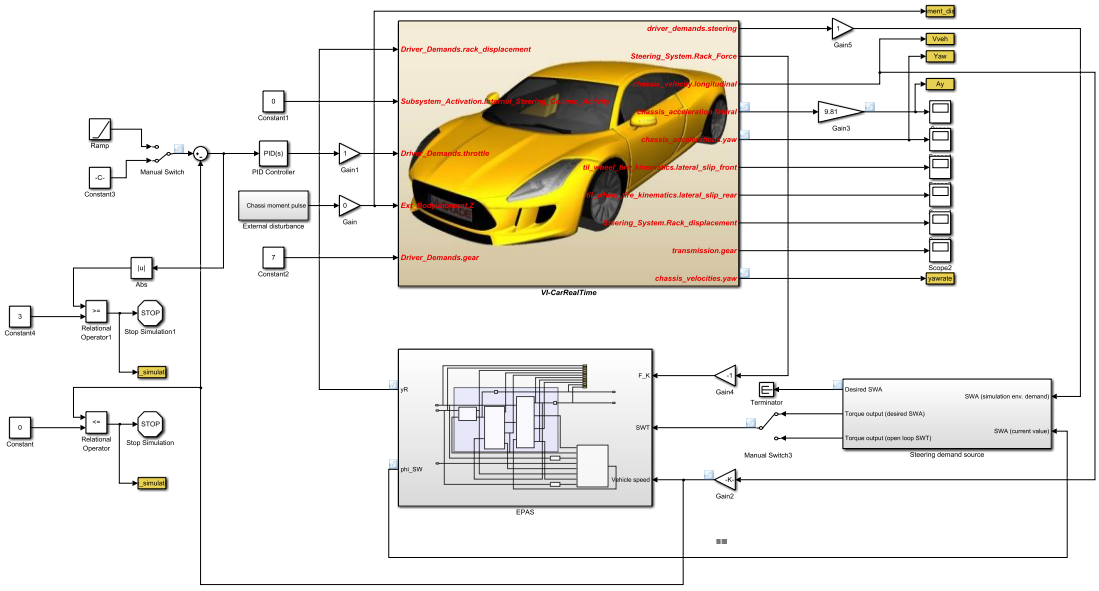

Fig 8. Screenshot of the Simulink co-simulation environment with the EPAS model and CRT block present.

The data file from CRT containing the vehicle and driver information did not need the steering system to do what the driver model stated. This meant that a driving scenario generator could be created in Simulink to control the steering system during the simulation. The vehicle model was only looking at the rack lateral displacement as an input, disregarding the driver model, making it possible to either use the built-in driver model or any input created in Simulink. By setting this structure up, the full power of simulation automation was unlocked so that every simulation could be dictated from a MATLAB script, not needing a new CRT data file for every driving scenario. The driving scenario generator then acted as a driver model as it supplied the model with a steering wheel torque to achieve a specific level of steering wheel angle. A simple feedback controller was implemented to actuate the system and the result was an open loop driving scenario regarding the steering wheel angle, but the steering wheel torque was controlled in a closed loop. This is similar to how a normal driver operates the vehicle, controlling the torque to achieve the wanted steering wheel angle.

3.2.2 Driving scenarios

The objectives for this project contained a set of tests for the model. The purpose of the simulations was to verify the functionality of the model as well as investigating the system impact on vehicle dynamics regarding stability and preserved steering feel and driveability. The used scenarios will be described in the following sections.

3.2.2.1 Model verification

To ensure that the produced model conveys a realistic result during simulations, a more complex model was benchmarked. Since the models had different levels of complexity and utilized different solutions as well as contained different functions, the results were compared qualitatively. The forces and states, such as velocities and displacements, was required to be in the same magnitude and showing the same characteristics for the developed model as the complex model. Since an objective of the developed model was to enable studies on changing parameters and functionality, the results could be tuned to suit the complex model better if necessary. Therefore, the verification becomes less crucial without being unnecessary. The general model behaviour and dynamics becomes all the more important to verify. However, the results from this comparison will not be presented in the report due to secrecy reasons regarding the more complex model.

3.2.2.2 Vehicle stability and steering feel

An area of interest for research during this project was the trade-off between stability on vehicle level, due to the steering system dynamics, as well as driveability and steering feel. As vehicle speed is heavily influencing the stability of the vehicle, a test with increasing speed was used. During simulation, the input torque on the steering wheel was zero, allowing the vehicle to move freely. Every tenth second, an external yaw moment was applied to the vehicle body for a tenth of a second inducing a disturbance in the yaw rate. If the vehicle turns unstable, it does so at a certain velocity. This velocity can be identified as when the yaw rate of the vehicle is not damped out but rather starts to increase by itself, according to the general stability definition.

To couple this type of simulation to steering feel, an on-centre driving scenario was used. Using the same variable setting, the behaviour of mainly steering wheel torque versus steering wheel angle was assessed. These simulations together show the trade-off between stability and steering feel for a certain setting in the variables.

3.2.2.3 Controller function dependability

As the steering system controller and its inherent functions could be altered, the need to investigate the dependency on these functions and combinations of them arises. In the same way as described in section 3.2.2.2, simulations on stability and steering feel was conducted with different controller settings. To connect to the research done by Sakai, the mechanical friction was also used as a variable to investigate its effect on the system stability in a similar way as the controller functions (Sakai, 2014). This gave six variables to vary during the tests and thereby 64 possible scenarios. However, some functions are dependent on others and cannot be active without those functions. Therefore, a lower number of tests were required.

3.2.2.4 Frequency response

A mechanical system can often be investigated further by examining its frequency response. The frequency response is a test to produce the estimated transfer function of the system and to plot the Bode plot for it. This shows the system response to a range of frequencies. The response is given in a format of a gain and a phase. The input and the output are selected and the gain tells how much output is given for each input as well as for how long the response is lagging. In the automotive industry, a well-known test is to drive the car at a fixed speed and do either a ramped frequency input on the steering or a randomized input. The data is then analysed and shows, with corresponding numbers for coherence or validity of the estimation, the system behaviour. In simulation, the car can be run for a long time at the same speed and the frequency of the steering input can be ramped precisely to give a higher coherence for each frequency and also increase the maximum frequency content estimated.

3.2.2.5 Standardized testing for system documentation

To achieve an industry consistency, there are standards for testing, measuring and analysing steering system and vehicle dynamics data. These standards clearly specify the driving scenario and the way data should be created. For the project, these tests are valuable since it gives a clear connection as to what is done on the test tracks and in simulations across the world. The tests are also designed to capture important parts of the system dynamics which lowers the amount of creativity during simulation scope development. The standardized simulations were carried out accordingly to the standards in Table 1.

Table 1. The two ISO standard driving scenarios performed in the project.

Number	Defined by	Name
ISO 13674-1:2010	SWA	Road vehicles – Test method for the quantification of on-centre handling
ISO 17288-2:2011	SWT	Passenger cars – Free-steer behaviour – Part 2: Steering-pulse open-loop test method

4 Results

Since the EPAS system has two major moving parts, the steering column and the rack whose states are crucial for the dynamics of the system, the modelling of the system has been as a 2-DOF system. This means that there are two equations of motion, one on the steering column using the sum of torques and the rotational inertia to calculate rotational acceleration, the other one for the rack and its equivalent mass, with the motor inertia considered, to give rack lateral acceleration. The full motor dynamics is considered fixed as a part of the rack without compliance but coupled using a gear ratio as is the real case. The component that allows the two system parts to move in relation to each other is the torsion bar that is flexible. The torsion bar also provides the mechanical coupling of the two subsystems by the connecting force it exerts in both ways on each side. This gives three subsystems in the EPAS that captures not every part of the system dynamics but a significant and sufficient level of it. The difference in inertia between the both subsystems and the connection between them gives rise to the dynamics necessary to evaluate stability, steering feel issues as well as implementation of the controller for the EPAS. The controller performance can then be analysed without altering the physics of the model.

As a separate subsystem in the EPAS model, the controller is given. This means that exporting the EPAS model does not limit system performance, as the controller comes with the model block. Treating the controller in the same way as one of the mechanical parts of the model is slightly different to normal procedure but as the dynamics of the model, and the real system, depends heavily on the implemented controller strategy, the controller is equally important during simulation of the system characteristics. This led to the decision of incorporating the controller in the model plant.

4.1 Model interface

The developed steering system model has five connectors, three inputs and two outputs. The steering system modelled has a mechanical interface on both sides of the system and each interface is represented as one input and one output. The steering wheel has a position and a torque on it as the interface to the driver. This is modelled as a steering wheel torque input and a steering wheel angle output. The torque is the input and the angle is the response of the system. In the same way, the rack force is an input and the rack displacement is an output. A real mechanical interface thereby requires two modelled signals, the stimuli and the response. The fifth connection to the system is the vehicle velocity, as used by the controller to decide on, for instance, steering assist and damping. This input is treated as a data signal. The real steering system receives more signals such as safety data, arbitration data, and higher level functional data to name a few. This is not treated in this project.

Instead of having the steering wheel torque as an input, an extra degree of freedom could be added. A massless component could be given an angle as input and, connected to the steering column with a spring-damper interface, the input torque could be a result of this change in position. This interface could be used when simulating scenarios with a specified steering wheel angle instead of controlling the SWT to achieve the wanted SWA.

4.2 Model components

In this section, the components modelled after mechanical parts are discussed and explained. The general layout of the model is shown in Fig 9, picturing four main components where three are mechanical components and one is the controller and thus not a physical part.

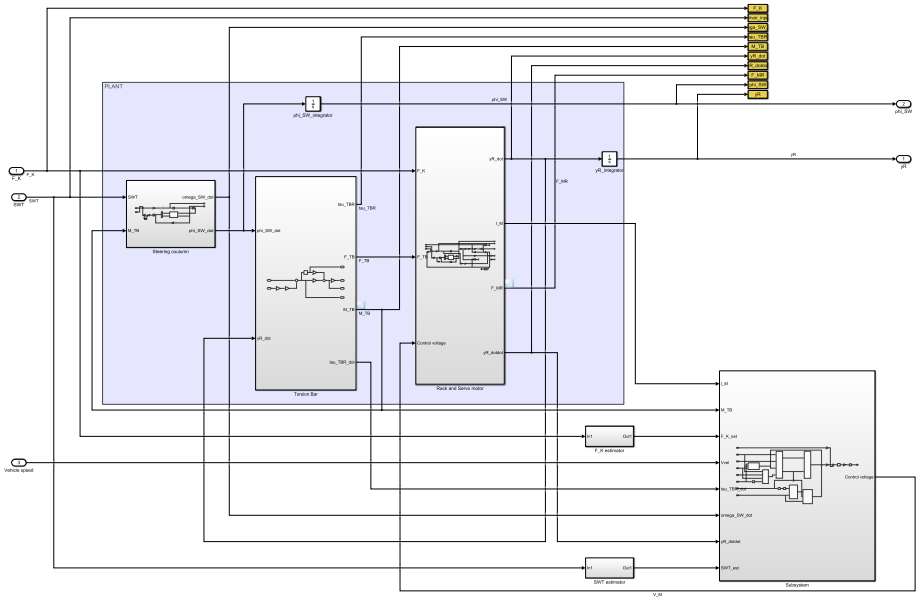

Fig 9. A screenshot of the EPAS model in Simulink.

4.2.1 Steering column block

The steering column is one of the two inertial systems present in the model. The model block has two inputs, the steering wheel torque and the torsion bar torque. These two torques together with the friction forces on the steering column are summed and gives the sum of torques on the rotational inertia. The sum is divided by the inertia giving the rotational acceleration which is integrated once for rotational velocity and once more for the steering wheel angle. A friction block with position and velocity as inputs was built. This block gives the frictional forces on the steering column based on its own states, thereby giving a loop in the system definition. This can be seen in Equation 2-4.

$$\dot{\omega}_{SW} = \frac{SWT - M_{TB} - F_{fric,SW}}{J_{SW}} \tag{2}$$

$$F_{fric,SW} = \left(\mathrm{F_{ESF}}\left(\phi_{SW}, \dot{\phi}_{SW}\right) + F_{damp,SW}\dot{\phi}_{SW}\right) r_{SW} \tag{3}$$

$$\phi_{SW} = \int \dot{\phi}_{SW} = \int\int \dot{\omega}_{SW} \tag{4}$$

The equation parameters and variables are listed in Table 2. The elastic spring friction element is explained in the next paragraph.

Table 2. List of parameters and variables.

Notation	Name	Value	Unit	Type
ω_{SW}	Steering wheel rotational velocity	-	[rad/s]	Variable
SWT	Steering wheel torque	-	[Nm]	Variable
M_{TB}	Torsion bar torque	-	[Nm]	Variable
$F_{fric,SW}$	Steering wheel friction	-	[Nm]	Variable
J_{SW}	Steering wheel inertia	0.048	[kgm^2]	Parameter
$\mathrm{F_{ESF}}$	Elastic spring friction force	-	[N]	Variable
ϕ_{SW}	Steering wheel angle	-	[rad]	Variable
$F_{damp,SW}$	Damping force steering wheel	-	[Ns/rad]	Variable
r_{SW}	Radius steering column friction lever	0.1	[m]	Parameter

4.2.2 Friction block

The friction forces used in this model block are based on equations given by Pfeffer (Pfeffer, Harrer, & Johnston, 2008). The speed dependent friction is given by a hyperbolic tangent function and some coefficients determining how quickly the friction builds up and to what level, shown in Equation 6. The friction force based on position is given by a more complex mathematical structure (Pfeffer, Harrer, & Johnston, 2008). Simply put, the friction force based on position is given by an exponentially degressive function in Equation 7. However, to capture the reversal dynamics, some logic operations needed to be developed. When the component subject to the friction stops and start moving the opposite way, the mathematical reference point for the friction calculation needs to change. The reference point is given by the current position minus the last reversal position plus the friction element deformation at this reversal point, since the deformation needs to unwind before the friction force switches sign. The friction element deformation is given by Equation 10 which is the inverse of the equation giving the friction force, Equation 7. The peak force at reversal gives the corresponding deformation that is included in the friction reference point. All equations, Equation 5-10, for the friction element are given here. This type of friction block is used in both the steering column block and the rack and motor block.

$$\mathrm{F_{ESF}}(\phi_{SW}, \dot{\phi}_{SW}) = \mathrm{F_{ESF,s}}(\phi_{SW}) + \mathrm{F_{ESF,d}}(\dot{\phi}_{SW}) \tag{5}$$

$$\mathrm{F_{ESF,d}}(\dot{\phi}_{SW}) = \tanh(\dot{\phi}_{SW} k_{d,stiffness})\, k_{d,limit} \tag{6}$$

$$\mathrm{F_{ESF,s}}(\phi_{SW}) = F_{limit}\left(1 - e^{-f_{ESF}\bar{\phi}_{SW} sign(\dot{\phi}_{SW})}\right) sign(\dot{\phi}_{SW}) \tag{7}$$

$$f_{ESF} = \frac{F_{limit}}{k_{ESF}} \tag{8}$$

$$\bar{\phi}_{SW} = \phi_{SW} - \phi_{SW,R} + \phi_{SW,B} \tag{9}$$

$$\phi_{SW,B} = -\frac{1}{f_{ESF}} \log\left(1 - \frac{F_{ESF,s,R} sign(\dot{\phi}_{SW})}{F_{limit}}\right) sign(\dot{\phi}_{SW}) \quad (10)$$

In Table 3, the corresponding parameters and variables are listed.

Table 3. List of parameters and variables.

Notation	Name	Value	Unit	Type
$F_{ESF,s}$	Elastic spring friction spring force	-	[N]	Variable
$F_{ESF,d}$	Elastic spring friction damping force	-	[N]	Variable
$k_{d,stiffness,SW}$	Damping stiffness coefficient SW	0.15	[-]	Parameter
$k_{d,stiffness,R}$	Damping stiffness coefficient Rack	15	[-]	Parameter
$k_{d,limit,SW}$	Damping limit coefficient SW	1.5	[Ns/m]	Parameter
$k_{d,limit,R}$	Damping limit coefficient Rack	15	[Ns/m]	Parameter
$F_{limit,SW}$	Friction force limit SW	1.5	[N]	Parameter
$F_{limit,R}$	Friction force limit Rack	210	[N]	Parameter
$k_{ESF,SW}$	Friction stiffness coefficient SW	12	[Nm]	Parameter
$k_{ESF,R}$	Friction stiffness coefficient Rack	1600000	[Nm]	Parameter

To find the reversal point, a simple logic function was created. It captures the value of the input, in this case the position, at the last zero crossing of its derivative which is the velocity. Another logic function needed for the friction element was the catch-block for the peak force at reversal. The operation of this function is shown in Fig 10. The output captures the present value as the signal shows any local minimum or maximum.

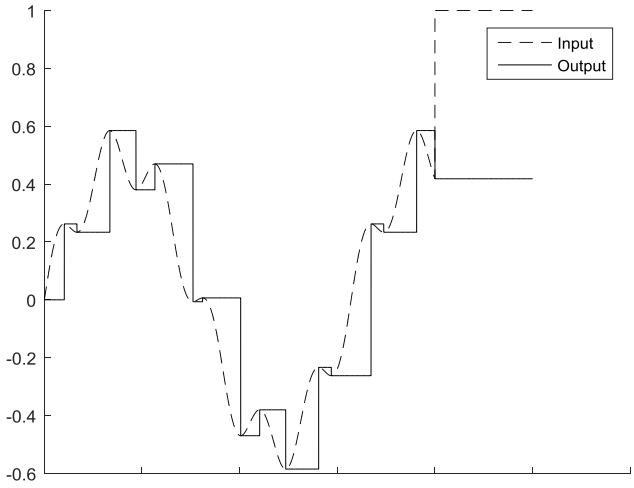

Fig 10. A benchmark test for the peak-force catch block. The block catches every local extreme value.

Together, the friction block gives a friction force characteristic according to Fig 11. The upper signal is the position signal, for instance the rack lateral displacement or the steering wheel angle, and the lower signal is the friction block output. The specific magnitude shown is not important for modelling understanding as the force level and its build-up is heavily dependent on application and thereby element parameters.

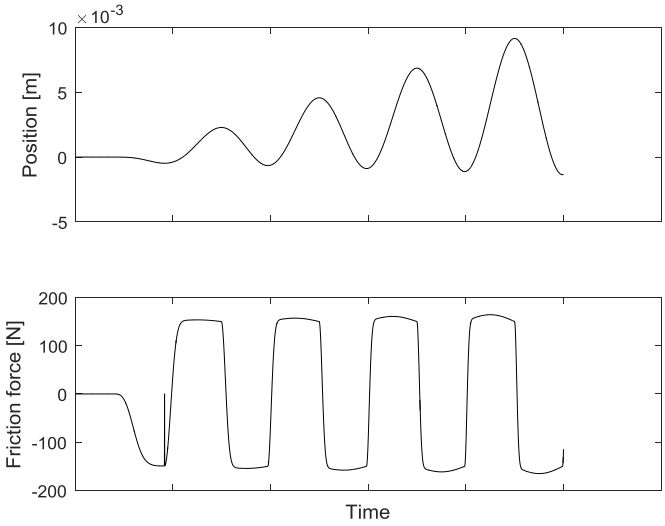

Fig 11. The friction block in a benchmark test. Input on top, output below.

4.2.3 Torsion bar block

The torsion bar is modelled by having the velocities of the ends of it as inputs and the response forces as outputs. The reason for choosing the velocities as inputs is to give information on the deformation rate, which is used for calculating the damping in the torsion bar, without the need to differentiate the position signals. The steering wheel rate minus the rack side velocity gives the rate of change in torsion bar deformation. The position difference of the ends is then given by integration of the deformation rate. Normally, the torsion bar is modelled with a slight damping due to losses in both the metal rod as such and the sensor and other components in the near surrounding. However, the spring force component is the governing factor and before calculating it, the rate of deformation is integrated. As the torsion bar is a sensor, the outputs from it are used for multiple reasons and several equivalent or dependent measures are given as outputs to the rest of the system. These are; the torsion bar deformation and deformation rate as well as the torsion bar torque and the resulting force on the rack, shown in Equations 11 and 12.

$$\dot{\tau}_{TBR} = \dot{\phi}_{SW} - \frac{\dot{y}_R nst}{r_K} \tag{11}$$

$$F_{TB} = \frac{M_{TB}}{r_{TB}} = \frac{c_{TB} \int \dot{\tau}_{TBR} + d_{TB} \dot{\tau}_{TBR}}{r_{TB}} \tag{12}$$

Again, the necessary values used in the above equations are listed below in Table 4.

Table 4. List of parameters and variables.

Notation	Name	Value	Unit	Type
τ_{TBR}	Torsion bar deformation	-	[rad]	Variable
y_R	Rack lateral displacement	-	[m]	Variable
nst	Steering ratio	15.9	[-]	Parameter
r_{TB}	Effective radius sensor pinion	0.0097	[m]	Parameter
r_K	Steering arm length	$r_{TB} * nst$	[m]	Parameter
F_{TB}	Rack force from sensor pinion	-	[N]	Variable
c_{TB}	Torsion bar rotational stiffness	145	[Nm/rad]	Parameter
d_{TB}	Torsion bar rotational damping	1.2	[Nms/rad]	Parameter

4.2.4 Rack and motor block

The rack and motor block is built in a similar fashion as the steering column with the addition of an extra force in the governing equation of motion. This extra force is the servo motor addition. The inputs for the rack and motor block are the tie rod forces and the rack force from the torsion bar or sensor pinion together with the control voltage to the servo motor. The rack motion is given by the sum of the two input forces, the motor force and the friction force on the rack divided by the equivalent rack mass. The friction force is calculated in the same way as for the steering column friction block.

The servo motor force is given by the current in an electric circuit model. The model is given by the sum of voltages coming from; the control voltage, the counter-electromotive force (CEMF or Back EMF) and the voltage loss due to the circuit resistance. The CEMF is a loss in voltage to the circuit based on the motor velocity, similar to a linear drag loss. At a certain motor speed, the voltage drop from the CEMF is equal to the actuating voltage, resulting in a no-load speed as the motor cannot produce any net force since there is no driving voltage left. The net voltage divided by the motor inductance gives the rate of change in motor current which is integrated. The current at any time multiplied by the motor torque coefficient gives the torque supplied by the motor. This torque is multiplied by the gear ratio giving the force on the rack which comes into the equation of motion for the rack and motor unit. This force is also given as an output in this model block for data acquisition purposes.

Having all four forces in the sum of forces for the equation of motion, the net force is divided by the rack equivalent mass. This mass is given by Equation 1, derived using the relationship of the gear ratio effect on the motor inertia. The result, and output from the block, is the rack acceleration and velocity which gives, together with the tie rod kinematics, the wheel steering angle after another integration. The rack velocity also determines the motor speed which is used for determining the CEMF at the next data point. The equations for the rack and motor blocks are given below, Equation 13-19.

$$y_R = \int \dot{y}_R = \int\int \ddot{y}_R \tag{13}$$

$$\ddot{y}_R = \frac{F_{TB} + F_K + F_M - F_{fric,R}}{m_R + \left(\frac{J_M}{r_M^2}\right)} \tag{14}$$

$$F_{fric,R} = \mathrm{F_{ESF}}(y_R, \dot{y}_R) + \dot{y}_R \left(F_{damp,R} + \left(\frac{F_{damp,M}}{r_M^2} \right) \right) \tag{15}$$

$$F_M = \frac{T_M}{rM} \tag{16}$$

$$T_M = I_M K_T = \int \dot{I}_M \, K_T \tag{17}$$

$$\dot{I}_M = \frac{V_M - K_E \frac{60}{2\pi} \frac{\dot{y}_R}{r_M} - I_M R_M}{L_M} \tag{18}$$

$$F_K = -F_{tyre,lat} \frac{t_{tyre} + t_{caster}}{r_K} \tag{19}$$

Table 5 lists the used parameters and variables for Equations 13-19. The motor pinion effective radius is smaller than reasonable due to that it is an effective radius given by the ratio in the two gear ratios connecting the servo motor to the rack. The result is a radius that is smaller than can be achieved in a single gear ratio step.

Table 5. List of parameters and variables.

Notation	Name	Value	Unit	Type
F_K	Rack force from tie rods	-	[N]	Variable
F_M	Rack force from servo motor	-	[N]	Variable
$F_{fric,R}$	Rack friction	-	[N]	Variable
m_R	Rack mass	3	[kg]	Parameter
J_M	Servo motor inertia	0.00021	[kgm^2]	Parameter
r_M	Effective radius motor pinion	0.00036	[m]	Parameter
$F_{damp,R}$	Rack damping	2.4	[Ns/m]	Parameter
$F_{damp,M}$	Motor damping	0.000005	[Ns/m]	Parameter
T_M	Servo motor torque	-	[Nm]	Variable
I_M	Servo motor current	-	[A]	Variable
K_T	Torque coefficient	0.04	[Nm/A]	Parameter
V_M	Servo motor control voltage	-	[V]	Variable
K_E	Speed coefficient	0.0044	[Vs/rad]	Parameter
R_M	Servo motor resistance	0.06	[Ohm]	Parameter
L_M	Servo motor inductance	0.04	[mH]	Parameter

$F_{tyre,lat}$	Tyre lateral force	-	[N]	Variable
t_{tyre}	Pneumatic trail	-	[m]	Variable
t_{caster}	Caster/mechanical trail	-	[m]	Variable

4.2.5 Mechanical and electrical system model layout

The connections between the three major physical component blocks in the model (steering column, torsion bar, rack and motor) are entirely mechanical. The steering column and the rack and motor blocks only have forces or torques as inputs from the steering system interface or from the torsion bar, with the exception of the control voltage input to the motor. The outputs from these blocks are positions and their derivatives. These variables are given to the torsion bar and the interfaces as responses to the taken forces and torques. Yet again, the motor has an exception as it gives its measured current to the controller block for feedback on the torque provided by the motor. The controller on the other hand, has many inputs. These are electronic signals used for computing the reference motor torque to be provided. The steering system controller input signals are:

- Servo motor current
- Torsion bar torque
- Estimated tie rod force
- Vehicle longitudinal velocity
- Torsion bar deformation rate of change
- Steering wheel velocity
- Rack acceleration
- Estimated steering wheel torque

4.2.6 Steering system controller

The controller for the EPAS model has multiple internal functions or blocks. The general layout can be seen in Fig 12. The components are listed below and explained in more detail in section 4.3.

- Basic assist (BA)
- Virtual model (VM)
- Active damping (AD)
- Feedback control (FB)
- Feedforward control (FF)
- Active return (AR)

The controller layout is normally called a 2-DOF controller (Åström & Wittenmark, 1996). There are four blocks giving reference states or force requirements (BA, VM, AD, AR) and two functions for ensuring that these requirements are met. The basic assist force is also passed directly through to the sum of required forces as this is necessary for steady state operation where the other references should be zero. The steering system would then enter an equilibrium. The required force is multiplied with the motor gear ratio, to attain the required torque, and connected to a PID-controller with the actual motor torque as a feedback parameter. The PID-controller gives a control voltage that is saturated to a maximum absolute value of 12 V as the vehicle electric circuit is limited in voltage supply.

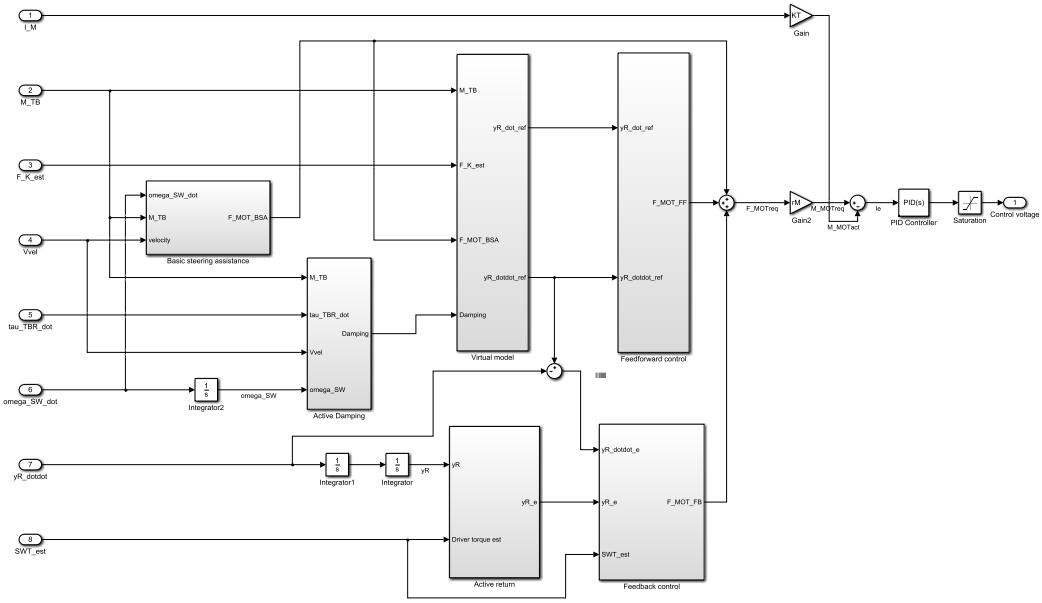

Fig 12. The controller block shown as a screenshot from Simulink.

4.3 Steering system controller functions

This project is limited in level of detail regarding the controller produced and the resulting solution is therefore not a fully developed system controller. The individual parts of the controller will be discussed here, nevertheless.

4.3.1 Basic assist

The function Basic Assist is in a sense a traditional boost-curve. That means that for a given torsion bar deformation, thereby torsion bar torque, an assist force is calculated (Harrer & Pfeffer, 2017). This force can be calculated by simple equations or, as is the normal case in the automotive industry, by a look-up table that can be edited, thus giving the ability to tune the assist function. Instead of shaping hydraulic valves as was the method with the HPAS system, the tuning is altered directly while inside the car, through a computer interface. The assist force is provided directly to the motor but it is also included in some other controller components.

In the basic assist part of the controller, a function for adding hysteresis was implemented as well. When approaching the peak steering in a manoeuvre, the steering wheel torque should drop slightly (Petersson, 2018). This behaviour gives a controlled return of the steering to zero steering angle and emulates a resisting friction force that can be tuned. More importantly, it demands a lower effort from the driver in steady state cornering which is crucial for driving comfort. This decrease in torque also gives room for a new torque build up, should the driver decide to increase the steering wheel angle, meaning that the increasing response torque does not feel too high or resisting. The peak steering torque is detected with a logic function, shown in Fig 13, included in Equation 21. This gives a square signal that by using two first order transfer functions first control the amplitude and phase of the hysteresis build-up and secondly smoothens it. The below equations that are not describing the hysteresis build-up shows the level of servo assist and the weighting of it. All equations for the basic assist function can be seen below, Equations 20-25.

$$F_{M,req,BSA} = F_{M,hysteresis} + F_{M,linear} + F_{M,quadratic} \tag{20}$$

$$F_{M,hysteresis} = k_{1,hyst}\mathrm{TF2}\left(\mathrm{TF1}\left(sign(M_{TB})\mathrm{Hyst}_{\mathrm{detection}}(M_{TB})\right)\right) \tag{21}$$

$$\mathrm{TF1} = \frac{k_{2,hyst}}{k_{3,hyst}s + k_{4,hyst}} \tag{22}$$

$$\mathrm{TF2} = \frac{1}{0.2s + 1} \tag{23}$$

$$F_{M,linear} = \frac{M_{TB}}{c_{TB}} k_{lin,servo} \tag{24}$$

$$F_{M,quadratic} = sign(M_{TB})\left(\frac{M_{TB}}{c_{TB}} k_{1,quadratic}\right)^2 k_{2,quadratic}\left(1 - \frac{V_{veh}}{70}\right) \tag{25}$$

The values used after tuning of the controller as well as variables for the above equations are shown in Table 6.

Table 6. List of parameters and variables.

Notation	Name	Value	Unit	Type
$F_{M,req,BSA}$	Required force basic steer assist	-	[N]	Variable
$F_{M,hysteresis}$	Required force hysteresis	-	[N]	Variable
$F_{M,linear}$	Required force linear servo	-	[N]	Variable
$F_{M,quadratic}$	Required force quadratic servo	-	[N]	Variable
$k_{1,hyst}$	Hysteresis coefficient	$0.5/r_{TB}$	[-]	Parameter
$k_{2,hyst}$	Hysteresis coefficient	12	[-]	Parameter
$k_{3,hyst}$	Hysteresis coefficient	1.5	[-]	Parameter
$k_{4,hyst}$	Hysteresis coefficient	1	[-]	Parameter
$k_{lin,servo}$	Linear servo coefficient	60000	[-]	Parameter
$k_{1,quadratic}$	Quadratic servo coefficient	15	[-]	Parameter
$k_{2,quadratic}$	Quadratic servo coefficient	10000	[-]	Parameter
V_{veh}	Vehicle longitudinal velocity	-	[m/s]	Variable

In Fig 13, the layout of the component providing the basic steering assist function with the hysteresis activation is shown.

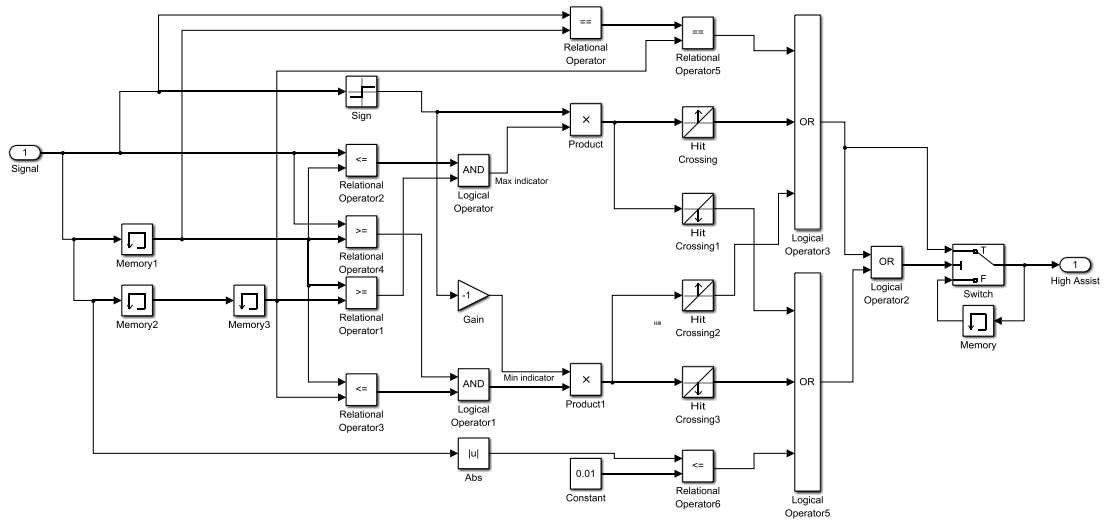

Fig 13. The logic layout in the hysteresis detection block, shown in Simulink.

The response of the component subject to a given input can be seen in Fig 14. The top signal is the input and the bottom signal is the output. The output has a positive edge as the input approaches a local maximum and a negative edge when approaching a minimum.

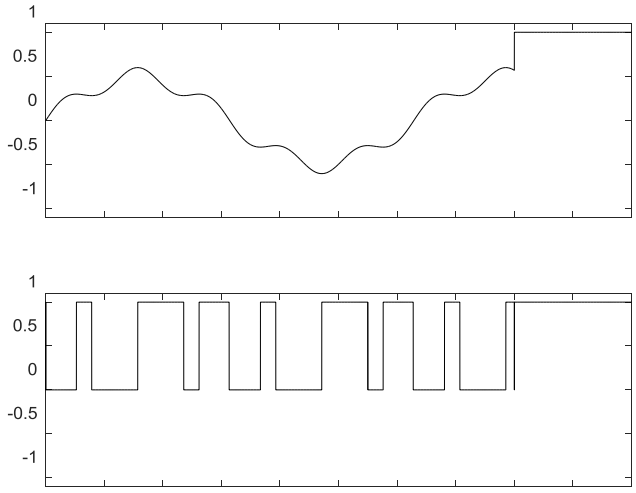

Fig 14. The input (top) giving the result (bottom) of for logic block.

4.3.2 Virtual model

Since the motor inertia is enlarged by the motor transmission giving an equivalent rack mass of approximately 1500 kg, the system needs a controller strategy to enhance the insufficient response. This has been done by implementing a model follower strategy (Abe, 2015). The EPAS system is set to follow the mechanical response of a virtual model that has the wanted, apparent forces as inputs (Chugh, Chen, Klomp, Ran, &

Lidberg, 2017). The estimated forces are applied to a fictitious mass that is set to a significantly lower value than the real equivalent mass. The rack acceleration is calculated and gives a reference movement, mimicking a HPAS or an unassisted system, that the real rack should follow, given in Equation 26. This effectively lowers the inertia in the system as the real rack, ideally, moves as a light rack. The desired rack mass acts as a tuning parameter for inertia compensation, that is, a lower desired rack mass means a high inertia compensation. Inertia compensation is a term describing the method of lowering the effective inertia of the steering system by amplifying the rack movements using the servo motor power actively. However, there is a lower limit on the desired rack mass set to the fictitious model, as the servo motor cannot imitate a too low mass. This virtual rack is the foundation for the virtual model block, being a reference generator block. The input forces to the virtual model are:

- Basic assist force
- Torsion bar force on rack
- Estimated tie rod force
- Active damping force

$$\dot{y}_{R,ref} = \int \ddot{y}_{R,ref} = \int \frac{\left(\frac{M_{TB}}{r_{TB}} + \widehat{F_K} + F_{M,req,BSA} - AD\right)}{m_{R,des}} \tag{26}$$

Below, the variables and parameters introduced are given in Table 7.

Table 7. List of parameters and variables.

Notation	Name	Value	Unit	Type
$y_{R,ref}$	Reference rack lateral displacement	-	[m]	Variable
AD	Active damping	-	[N]	Variable
$m_{R,des}$	Desired rack mas	10	[kg]	Parameter

4.3.3 Active damping

The purpose of the active damping is to add stability to the EPAS system, as the inertia coming from the motor induces instability to the system and the inertia compensation in the virtual model exaggerates the instability. Another requirement of the active damping is to create or shape a desired steering feel. The steering feel quality of the damping depends on its implementation. The amount of damping can be based on steering wheel angular velocity giving a dead feel in comparison to damping based on steering wheel torque. The latter can be tuned to stabilize the system significantly during small driver inputs and to intervene less at higher steering wheel torques, thereby increasing steering ability. The active damping is only fed into the virtual model, in order to create as pure a rack movement as possible, Equation 27-30.

$$AD = M_{TB,damp} + TBR_{damp} + Main_{damp} \tag{27}$$

$$M_{TB,damp} = M_{TB}\text{LookUp}_{\text{table1}}(|M_{TB}|)k_{MTB,damp} \tag{28}$$

$$TBR_{damp} = -\dot{\tau}_{TBR} k_{TBR,damp} \tag{29}$$

$$Main_{damp} = \text{LookUp}_{\text{table2}}\left(\left|\omega_{SW} k_{main,damp1}\right|, \left|V_{veh} k_{main,damp2}\right|\right) sign(\omega_{SW}) k_{main,damp3} \tag{30}$$

The parameters because of the tuning process and the corresponding variables are shown in Table 8.

Table 8. List of parameters and variables.

Notation	Name	Value	Unit	Type
$M_{TB,damp}$	Torsion bar torque damping	-	[-]	Variable
TBR_{damp}	Torsion bar torque rate damping	-	[-]	Variable
$Main_{damp}$	Main damping	-	[-]	Variable
$k_{MTB,damp}$	Damping coefficient	120	[-]	Parameter
$k_{TBR,damp}$	Damping coefficient	3000	[-]	Parameter
$k_{main,damp1}$	Damping coefficient	3	[-]	Parameter
$k_{main,damp2}$	Damping coefficient	1/15	[-]	Parameter
$k_{main,damp3}$	Damping coefficient	100	[-]	Parameter

4.3.4 Feedback control

To follow the references set for the system, a feedback controller was used to minimize the difference between the real rack movement and the movement of the virtual model. The controller used was a PI controller with fixed parameters. To improve the performance of the controller, these parameters could be given dynamic values to give a more flexible system behaviour regarding responsiveness and stability. The equations in the feedback control block are given below, Equation 31-34. The rack lateral displacement error is given by the active return function, shown in Section 4.3.6.

$$F_{M,req,FB} = \text{PID}\left(y_{R,error}\right) + \text{PID}\left(\text{TF3}\left(\ddot{y}_{R,error}\right)\right) k_{arbitration} \tag{31}$$

$$\text{TF3} = \frac{1}{0.1s + 1} \tag{32}$$

$$k_{arbitration} = \text{IF}\left(\widehat{SWT} \neq 0\right) \tag{33}$$

$$\ddot{y}_{R,error} = \ddot{y}_{R,ref} - \ddot{y}_{R} \tag{34}$$

The variables used are shown in Table 9.

Table 9. List of parameters and variables.

Notation	Name	Value	Unit	Type
$F_{M,req,FB}$	Required force feedback controller	-	[N]	Variable

$y_{R,error}$	Rack lateral displacement error	-	[m]	Variable
$k_{arbitration}$	Arbitration variable	-	[-]	Variable

4.3.5 Feedforward control

To enhance the system agility and increase responsiveness, a feedforward controller was built in together with the feedback controller giving a 2-DOF controller. The feedforward block calculates the force needed to achieve the reference acceleration, given by the virtual model, with the real rack and sends this force directly to the motor controller. The purpose of this method is to directly achieve an acceleration that is close to the reference value, relieving the feedback controller effort. The force needed is based on the real rack mass and the equivalent motor inertia on the rack, given in Equation 35. These parameter values must be known and if they are deviating slightly, which is common in reality, the error in the force fed forward will be significant. This makes the feedforward method sensitive and unreliable in application. For the final design of the controller, the feedforward part was not used meaning that the entire motor force required came from the feedback controller and the pure basic assist force.

$$F_{M,req,FF} = \ddot{y}_{R,ref}\left(m_R + \left(\frac{J_M}{r_M^2}\right)\right) \tag{35}$$

The corresponding variable is shown in Table 10.

Table 10. List of parameters and variables.

Notation	Name	Value	Unit	Type
$F_{M,req,FF}$	Required force feedforward controller	-	[N]	Variable

4.3.6 Active return

Due to the system mechanics, the aligning torque from the tyres on the knuckle giving the tie rod forces is not enough to bring the steering back to centre sufficiently, when driving slowly or in low speeds. To help the car align the steering, an active return function was added. When at low steering wheel torques, the function adds a resisting torque bringing the steering wheel back to zero angle by utilizing an error signal for the feedback controller block, Equation 36. When the driver lets go of the steering wheel, this function is given the main control over the system as the active return and the basic steering assist works in the opposite directions, therefore making the controller end up in equilibrium off-centre otherwise. Active return functions largely affect the steering feel and it is therefore important to tune the characteristics of it (Petersson, 2018). In this project however, the active return function mainly contributes with some stabilization of the steering system and therefore, the on-centre feel with regards to the function is not regarded to great extents.

$$y_{R,error} = \left(\text{Saturation}_0^1\left(\left|\widehat{SWT}\right|\right) - 1\right)y_R \tag{36}$$

4.4 EPAS system simulation results

In this section, all the simulated results are shown. Mainly by showing tables of data and plots of different relations. The results are analysed and discussed in Chapter 5.

4.4.1 Controller function dependability

As mentioned in Method, a study with varying controller functions activated was performed. The study, using 24 combinations of different controller functions activated, was performed on stability and steering feel. Nine of these setups will be used for further investigation as not all 24 are interesting. Out of these 24 combinations, six shows instability and they are all included in the nine further investigated cases. The other three cases are interesting based on steering feel performance or due to interesting system setups. In Table 11, the nine test results are shown, whether or not they are unstable and their corresponding critical speed, i.e. the speed at which they turn unstable. Note how the added mechanical friction between test 7 and 8, does not affect the system stability greatly. However, adding active damping in test 12 gives stability for all possible vehicle speeds. In test 23, the active damping creates a stable vehicle without friction in the system.

Table 11. The test setup for the controller function dependability.

Test number	AR	AD	BSA	FB	VM	Friction	Stable	V_{crit} [km/h]
1	0	0	0	0	0	0	-	153
5	0	0	1	0	0	0	-	126
7	0	0	1	1	1	0	-	<100
8	0	0	1	1	1	1	-	125
12	0	1	1	1	1	1	Yes	-
19	1	0	1	1	1	0	-	<100
20	1	0	1	1	1	1	-	127
23	1	1	1	1	1	0	Yes	-
24	1	1	1	1	1	1	Yes	-

A typical plot of yaw rate for the stability test is shown in Fig 15, where the event of instability starts when the induced yaw rate does not reduce but starts to increase. This occurs at 65 seconds. Every unstable setup shows the same type of behaviour and every stable system setup shows continuously decreasing yaw rate signal after every induced disturbance. The settling time, however, increases with added vehicle speed for any given fixed setup.

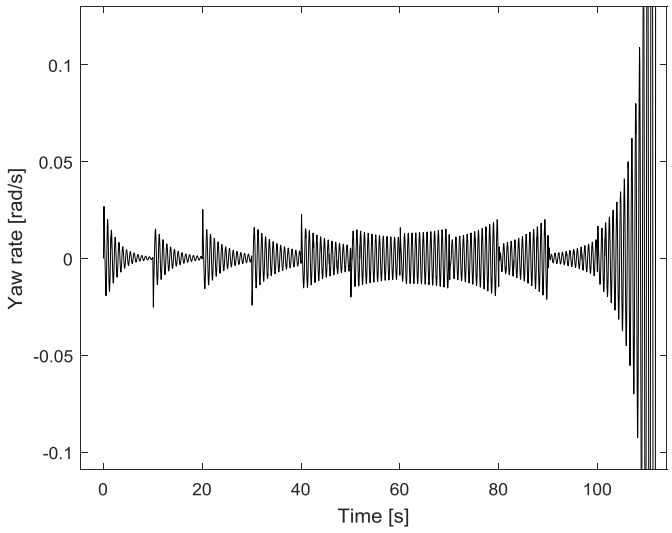

Fig 15. Yaw rate versus time for an unstable setup.

In order to investigate how well the system settings worked with regards to driveability and steering feel, on-centre tests were performed as well. The relationship used to analyse this data is the relation between the steering wheel torque and the steering wheel angle. The most important factor to notice in Fig 16 is the smoothness of the curves as these setups are reasonable to utilize in a vehicle based on steering feel. However, Fig 16b shows the steering feel for the unstable setup shown above in Fig 15. Whether these steering feels are good from a driver's point of view is left out due to the limitation on subjective steering feel assessments. A desired steering feel is thereby indicated by the lack of irregular steps, vibrations and other unsmooth characteristics.

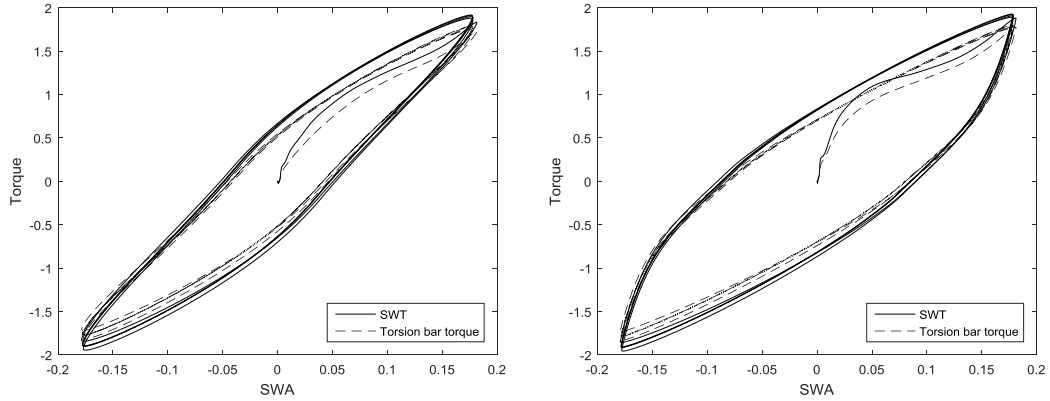

Fig 16. Two setups showing a desired steering feel due to linearity and smoothness. Left (a), right (b).

Fig 17 shows a steering feel behaviour that has a stable operation in the stability test but the steering feel is not desirable, mainly due to an unnatural shape with steps as well as vibrations.

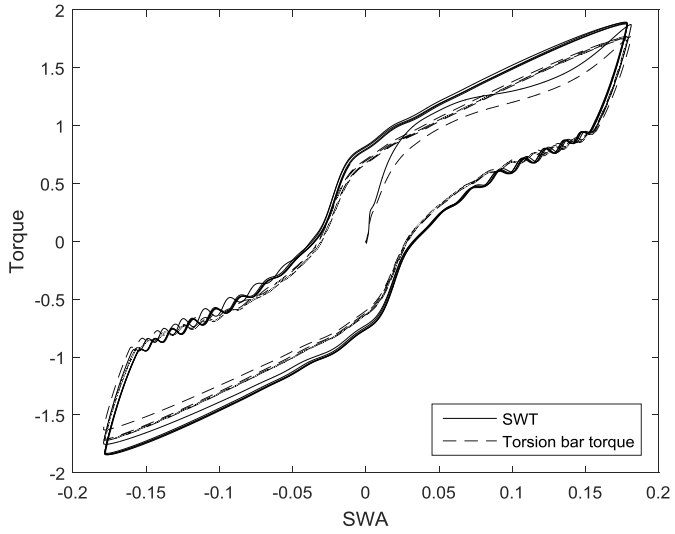

Fig 17. Unwanted steering feel due to steps and vibrations.

4.4.2 System and vehicle stability analysis

The simulations for further stability investigation regarding steering system impact was all done using all controller functions except controller feedforward. The variables in this study was the level of main damping, the servo motor gear ratio as well as the virtual model reference rack mass or the level of inertia compensation. A simple combination of tests was conducted where each variable was varied at a time. The target of the study was to identify the effect the variable had on critical speed. In Table 12, the run variable data is shown together with the critical speed result. Since not all variable combinations gave instability, the settling time for yaw rate at 250 km/h was noted when available as well. A higher number indicates a lower stability margin. This data is also shown in the table. Note that for an increasing desired rack mass, or decreased inertia compensation, the stability of the vehicle increases.

Table 12. Simulated test setups and results.

$m_{R,des}$ [kg]	Stable	Critical speed [km/h]	Settling time at 250 km/h [s]
10	-	235	-
40	-	238	-
70	-	247	-
100	-	260	8
400	Yes	-	4.5
700	Yes	-	3.5
1000	Yes	-	2.5

The reason for the instability in these tests, whereas the same function combination setting produced a stable result with the same desired rack mass, is the lowered damping in these tests. The lowered damping was used to create the instability, thereby giving the opportunity to investigate the inertia compensation effect on stability. With the

normal damping, all these tests would have been stable. In Table 13, the damping as the varied parameter is shown. The lowest desired rack mass was used throughout these tests. For an increased damping, the stability increases. With no damping, the stability disappears as was seen in the function dependency tests as well.

Table 13. Simulated test setups and results.

$Main_{damp}$	Stable	Critical speed [km/h]	Settling time at 250 km/h [s]
0	-	<100	-
10	-	240	-
20	-	245	-
30	-	255	Remaining oscillations
40	-	256	>20
50	-	301	12

An observation that could be made during these tests were that when instability occurred, the car only started oscillating slightly more. The vehicle did not turn around or "lose control". This had the effect that the car was clearly unstable or the yaw rate was increasing, that is, but it kept on going throughout the test. The damping coefficient of 30 had remaining oscillations before turning unstable, as well, meaning that there was no real settling time. Only a minimum value of oscillations reached. In Table 14, the results from tests varying the servo motor gear ratio are shown. However, there are no clear trends to observe in the data since the trends are either too small or not significant. There is a difference between using the controller or not as the tests without the controller were stable which connects to the controller function dependency, again.

Table 14. Simulated test setups and results.

Motor gear ratio variation	Controller	Stable	Critical speed [km/h]	Settling time at 250 km/h [s]
+50%	Yes	-	225	-
+25%	Yes	-	235	-
Standard	Yes	-	239	-
-25%	Yes	-	235	-
-50%	Yes	-	244	-
+50%	No	Yes	-	1.8
+25%	No	Yes	-	1.6
Standard	No	Yes	-	1.5
-25%	No	Yes	-	1.6
-50%	No	Yes	-	1.6

4.4.3 Frequency response for system characteristics

The yaw rate gain of the vehicle with the developed steering system shows the system behaviour well. The wheel angle to yaw rate can be seen in Fig 18, where the characteristics of a typically understeered but responsive vehicle can be observed. Normally, a generic vehicle would have a peak yaw rate gain, in degrees per second for every 100 degrees of steering wheel angle, of around 25-50, depending on the velocity. As the steering system should, in this case, only provide a reliable steering functionality on the vehicle, this study mostly serves as a verification on the model accuracy and authenticity. The coherence of the estimated transfer function is at most two percent off maximum correlation. The exact values in the analysis can unfortunately not be shown due to secrecy in the vehicle characteristics.

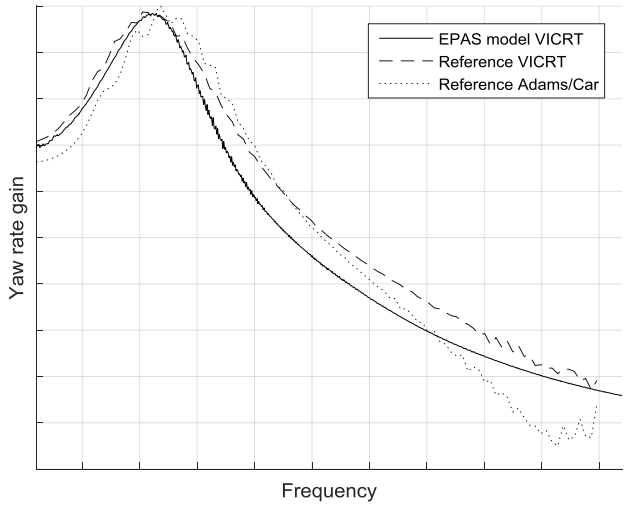

Fig 18. The yaw rate gain for steering wheel angle input from the estimated transfer function.

4.4.4 Standardized testing for system documentation

To clearly observe and document the performance of the modelled steering system and its controller, two ISO-tests were performed.

4.4.4.1 Weave test (ISO 13674-1:2010, IDT)

The weave test is an on-centre test utilizing a steering input in the shape of a sinusoidal curve, as implemented here, or similar. A number of measurements are available and a selection of them are shown in Table 15. Three setups in the controller has been simulated, as can be seen in Fig 19 and Fig 20. These figures show the SWT versus SWA relationship for setups with all controller functions, the active return switched off as well as for the setup with hysteresis switched off. There is a clear differentiation between the results as the active return clearly tightens the hysteresis which can also be observed in Table 15, showed by the hysteresis measurements or abscissa dead band numbers.

Table 15. Results for the on centre tests.

Figure	Function	Abscissa dead band [deg]	Ordinate dead band [Nm]	Steering stiffness [Nm/deg]
Fig 19	No AR	12	2	0.16
Fig 20a	All functions	7.5	1.6	0.2
Fig 20b	No hysteresis	2	0.4	0.16

The hysteresis almost disappears without the hysteresis function activated, both showing the system sensitivity and the importance and functionality of the hysteresis function in the controller. Fig 19 shows the result using all controller functions except active return.

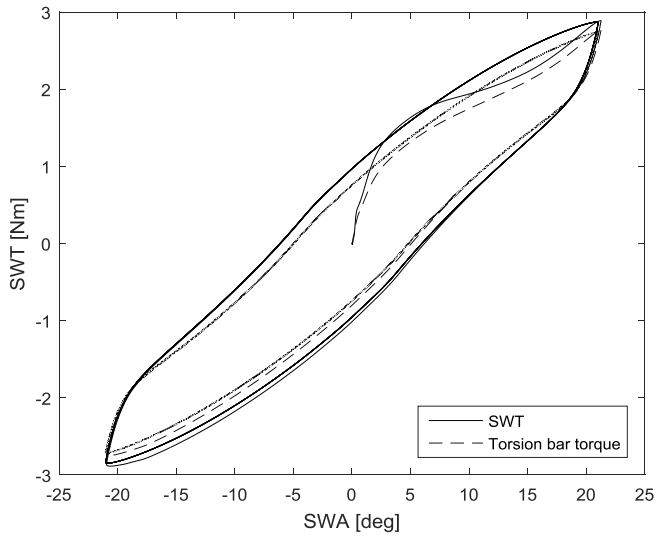

Fig 19. SWT versus SWA for the on centre test without active return.

Fig 20a and Fig 20b shows the results for all functions active and for the exception of hysteresis, respectively.

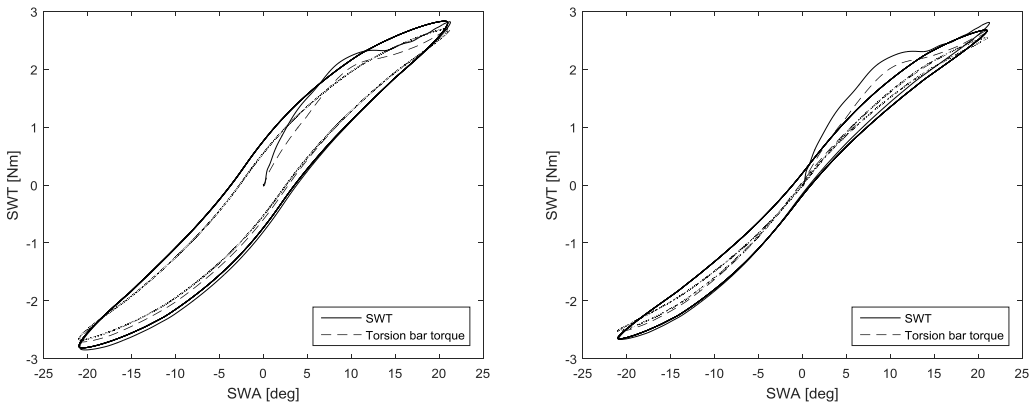

Fig 20. Two SWT versus SWA figures. Left (a), has all controller functions activated. Right (b), has the hysteresis deactivated.

Another interesting type of figure is the rack assistance force versus torsion bar twist. This kind of figure shows how much servo assist the motor applied for a given deformation in the torsion bar or steering wheel torque. In Fig 21 and Fig 22, the same test cases as used above can be seen. Again, the differences between the three cases are visible. This difference is the underlying reason for the results in the SWT vs. SWA figures. In the HPAS systems prior to the EPAS systems, the torsion bar deformation gave a set assist force. This type of relation is called a Boost-curve. The following figures show this type of relation, in the specific test case, but for the developed EPAS model. Fig 21 shows the assist corresponding to Fig 19 above.

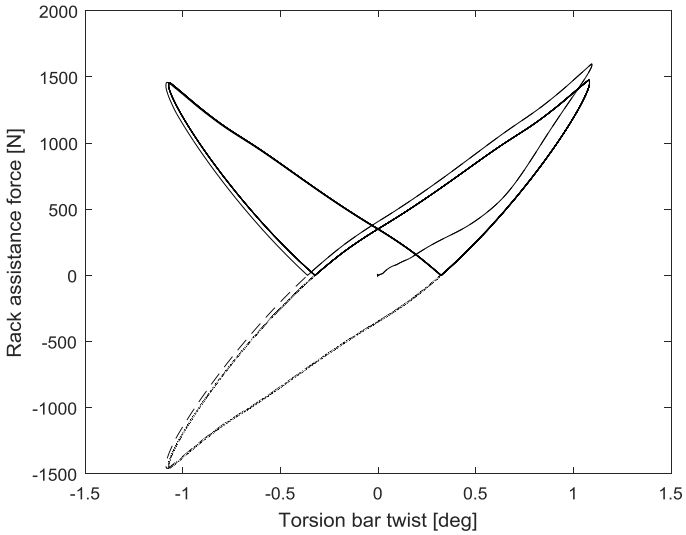

Fig 21. Rack assistance force versus torsion bar deformation, no active return.

Fig 22a and Fig 22b shows in the same way, the assist corresponding to Fig 20.

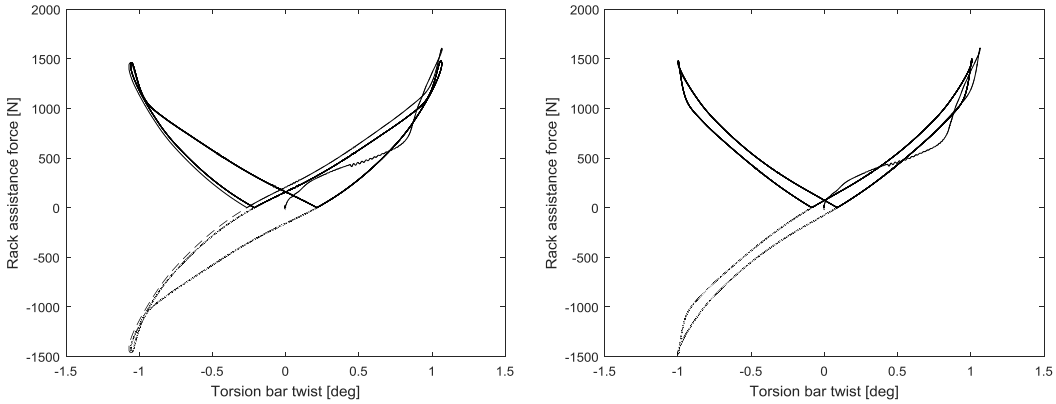

Fig 22. Rack assistance force versus torsion bar deformation. Left (a), all controller functions. Right (b), no hysteresis.

4.4.4.2 Steering-pulse open-loop test method (ISO 17288‑2:2011, IDT)

For the steering-pulse test, five certain levels of lateral acceleration should be achieved during the steer pulse. After the steer pulse, the steering wheel torque is set to zero, implying a no hands manoeuvre or a free steering wheel response scenario. The main reason for this specific test is to identify the settling time of the steering system and vehicle. A key aspect is also the ability of the steering system to return to straight ahead driving. In the portrayed Fig 23, the steering system fails to do this twice out of five runs, implying that the active return function is either not working or that its directive, as is more likely, is lost in arbitration and not given the priority to achieve the straight ahead driving. The two failed returns are the tests with the lowest initial lateral acceleration. The settling time for all tests are approximately 1 second.

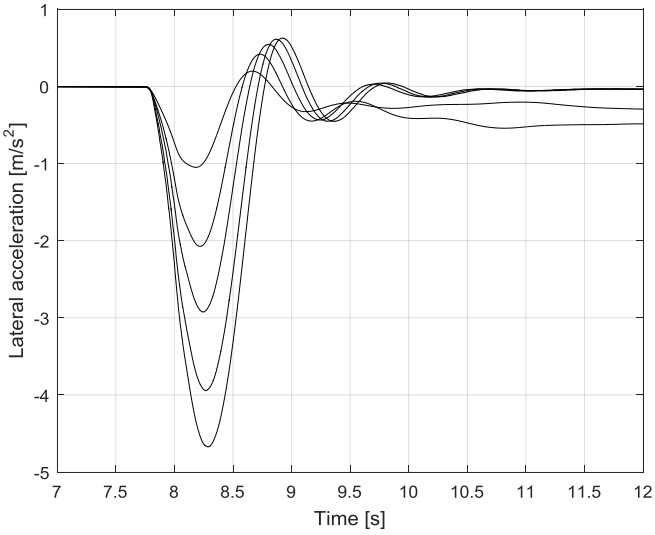

Fig 23. Lateral acceleration for the induced disturbance tests.

5 Analysis and discussion

5.1 The developed model

The developed model has been built according to the desired specifications. It has comparatively low computational requirements but still replicates the complexity, and mainly the inertia issue, of the steering system. The controller is limited in functionality, specifically its ability to handle different situations, as it might behave unexpectedly in certain scenarios. However, this area in the project was a clear delimitation as only basic functions were supposed to be developed and not a fully working controller for production use. Most importantly, the controller framework, which is in the same class as production units, enables the ability to further increase its capabilities and functionality. The model could potentially have been modelled using other methods but the result, the final version, fulfils the requirements and shows a high potential for further improvements. That should be considered a positive project outcome.

5.2 Controller function trade-off analysis

Regarding the stability of the vehicle based on different controller functions used but with fixed parameter values, there are clear indications on the importance of certain functions. In all unstable setups, active damping was turned off, showing its significant ability to produce a more stable vehicle unit. Comparing to the introduction of friction, the active damping makes the vehicle completely stable whereas the friction only increases the critical speed by a small margin. The level of friction and active damping does affect these differences but the characteristics are clear, since the amount of damping and friction used where the proper values used in the final model version. It is also clear that more functions for making the steering system more responsive decreases the stability (Chugh, Chen, Klomp, Ran, & Lidberg, 2017). Without any controller, the vehicle becomes unstable without friction but remains stable with friction (Sakai, 2014). There is a clear trend on a higher critical speed with added stability measures, as expected (Sakai, 2014).

5.3 System and vehicle stability analysis

Investigating the parameter sweep for stability further strengthens the observations of the decreased stability with increased responsiveness, or as in this case increased inertia compensation, confirming the results from literature (Chugh, Chen, Klomp, Ran, & Lidberg, 2017). For a higher desired rack mass, which is equivalent with a lower inertia compensation, used in the virtual model, the critical speed increases or alternatively, the settling time at 250 km/h reduces. To further show the trend, the settling time of the yaw rate at 125 km/h has been measured and plotted, shown in Fig 24. A clear trend is now depicted, showing the increased stability with decreased inertia compensation.

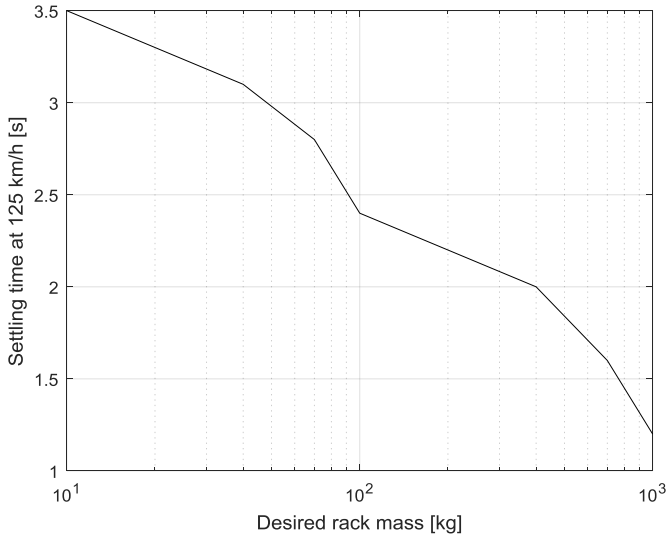

Fig 24. Settling time at 125 km/h for varying desired rack masses. A higher value means less inertia compensation.

The damping however, cannot be analysed in the same clear manor. When the vehicle reaches instability, the steering wheel rotational speed increases and so does the damping, meaning that the vehicle never turns properly unstable. This result was unexpected but completely reasonable. The same relation is applied to the vehicle velocity as a higher velocity gives, theoretically, a lowered stability but the damping on the steering system increases with vehicle velocity to counteract this phenomenon. For a higher damping, the critical speed increases as expected though. Having no damping is significantly more worse than reducing it multiple times in comparison to the highest tested value. Again, the settling time at 125 km/h for the varied damping tests is shown in Fig 25. The damping of 0 (given 10 as a result) was unstable and therefore never settled. For the clarity of the plot and its trend, a value of 10 seconds of settling time was given, instead of an infinite value as would be the case otherwise. The results show that a damping is crucial for stability but as the damping increases, there is only a marginal stability increment to be gained as the settling time levels out.

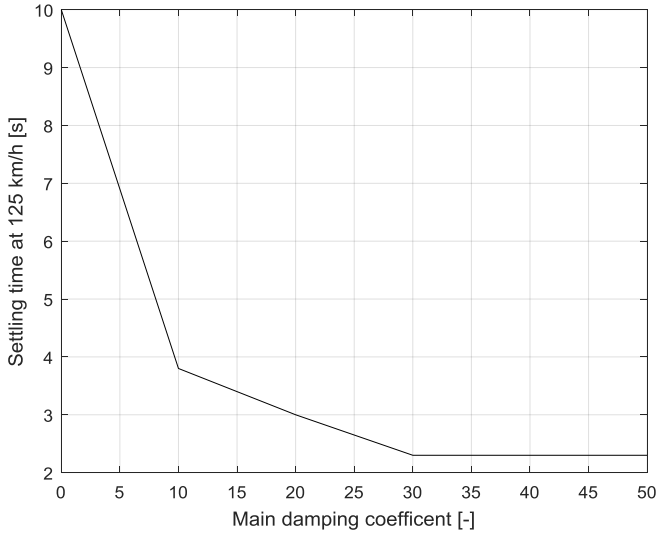

Fig 25. Settling time at 125 km/h for varied main damping.

The inertia is an issue that heavily influences the vehicle stability (Sakai, 2014). Changing the servo motor gear ratio directly alters the effective inertia and should therefore have an impact of the critical speed of the vehicle. With the controller activated, there is a slight trend towards a better result for lower gear ratios or lower inertia. The trend is not strictly increasing though, and the differences between the setups are smaller than expected for such high inertia differences. A 50 % drop in gear ratio means a 75 % drop in effective inertia according to Equation 1. With the controller turned off, the vehicle turns stable but the settling time does not change significantly with the varied gear ratio. The change in values might as well be measurement errors. This is the most unexpected result throughout the project as the vehicle instability should clearly be affected by this change.

To investigate this issue further, new simulations on vehicle stability without controller interaction and without mechanical friction were performed. A new relationship of critical velocity due to changes in equivalent rack mass was found, shown in Fig 26. This relationship clearly connects to the work done by Sakai (Sakai, 2014). A critical value of 325 km/h in the figure means that there was no instability using the corresponding setup, in the simulation.

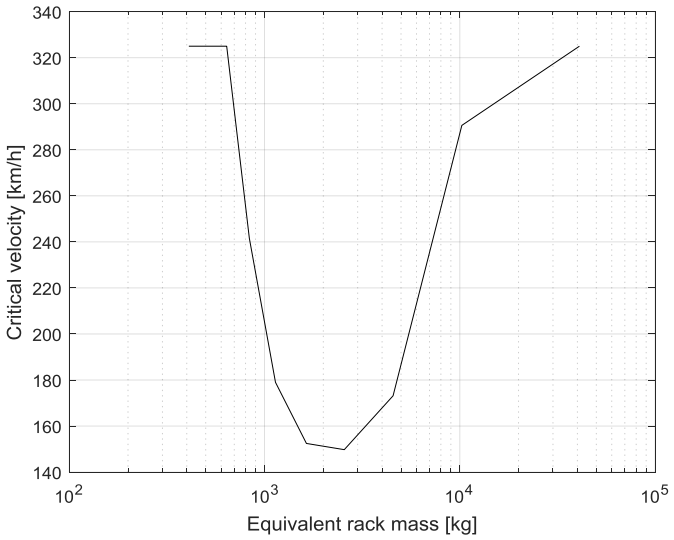

Fig 26. Vehicle critical velocity for varying equivalent rack masses. The steering controller and mechanical friction has been deactivated.

The settling time at 125 km/h was investigated as well, Fig 27, to show the level of stability for each equivalent rack mass. This measure includes the stable setups in the analysis as well as the unstable.

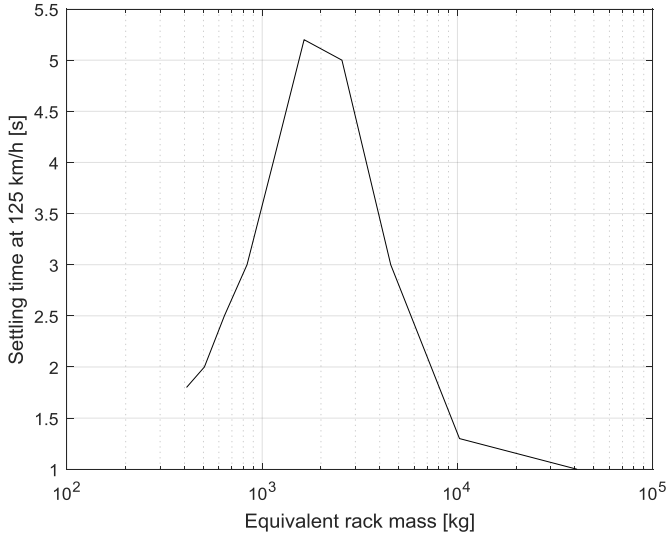

Fig 27. Settling time at 125 km/h for varying equivalent rack masses. The steering controller and mechanical friction has been deactivated.

The low settling time for low equivalent rack masses are expected and according to the literature (Sakai, 2014). The peak in settling time, or the minimum in Fig 26, is the standard inertia level in the model meaning that the worst setup is used. This is a level of inertia common in the industry, indicating the issues present when utilizing the EPAS system. The drop in settling time for higher inertias can be due to a lower steering system eigenfrequency than the vehicle eigenfrequency, producing separation between the frequencies and thus, limiting the stability issues. This solution is not viable for real vehicles, however, due to a too low responsiveness. The low responsiveness can be the cause to the stability as well. The tyres are still dampening the motions slightly and the high inertia of the steering system in this region (around 10 000-40 000 kg) might lock the response completely, rendering the possibly unstable system stable due to no response. This would be represented by positive system poles but a low amplitude for the response.

5.4 Frequency response for system characteristics

Comparing the generic vehicle response, from both Adams/Car and CRT, to the same vehicle equipped with the developed steering system model, the results show the preservation of the vehicle characteristics. The model cannot affect the vehicle response to great extents but this result shows a validity check for the developed model meaning that it performs as a normal steering system should.

5.5 Standardized testing for system documentation

5.5.1.1 Weave test (ISO 13674-1:2010, IDT)

The weave test results show the model flexibility in producing different steering feels. The parameters of the different functions can be tuned endlessly to create the desired steering feel. If there is an aspect that is not included in the controller, it could be expanded to give an even higher flexibility. Depending on the purpose of the model, it can be modified to suit the requirements. If the model should replicate a precise steering feel, it can be calibrated to do that. If it should be used to evaluate new settings or try new settings early in the development phases of vehicles, it provides the user with the required adjustability. A couple of illustrative tests were performed with changing parameters in the controller to adjust the shape of the SWT versus SWA plots. In Fig 28, the impact of the hysteresis rate can be seen, looking at high steering wheel angles and a 20 % drop and increase in hysteresis rate. The height of the hysteresis part around the torque reversal changes as the hysteresis rate is changed.

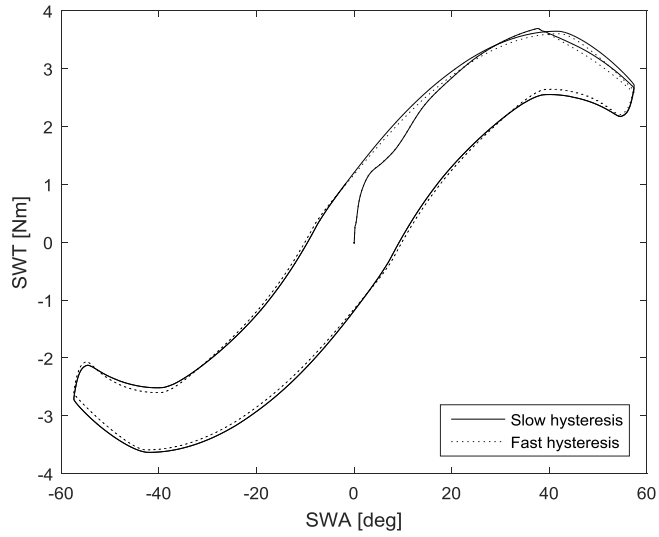

Fig 28. SWT versus SWA for a high steering wheel angle input. Two lines showing different hysteresis actuation rates.

For lower steering wheel angles, the hysteresis amount can be observed as Fig 29a has a lower abscissa dead band than Fig 29b. The amount of hysteresis has been decreased and increased by 20 %. The increase in hysteresis will feel as a higher friction in the system as the abscissa dead band measure is also called friction dead band.

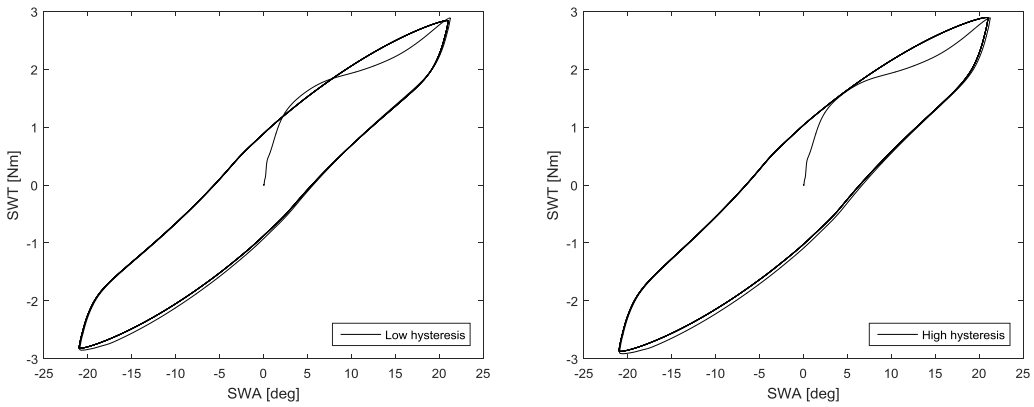

Fig 29. Two plots showing different magnitudes of hysteresis. Left (a), low hysteresis and right (b), showing a high hysteresis.

5.5.1.2 Steering-pulse open-loop test method (ISO 17288‑2:2011, IDT)

As can be seen in Fig 23, the active return does not work correctly. Further investigations in the controller operation during this type of scenario would be advantageous. However, the system response is clear and as expected, meaning that the model works as intended, mechanically. Unaffected by the level of initial lateral acceleration, the vehicle settles in approximately the same time. The amount of oscillations is also reasonable as there is only two or three big oscillations before the vehicle stops moving around (Petersson, 2018). The model thereby works in the same manner as would the real system.

6 Conclusions

Setting up the system to be modelled using simple but accurate physical equations, such as the equations of motion, leads to low computational requirements but a high level of model accuracy. This obviously require a simple enough system to be modelled. The dual-pinion EPAS can be resembled as two masses, coupled with a spring-damper interface and an extra inertia from the motor. Adding the motor torque, friction and the interface towards the driver and vehicle gives high enough complexity and accuracy in the model to use it for product development. It becomes a tool for setting requirements and verifying the fulfilment of them.

A key step in enabling the ability of the model to perform such tasks as aiding in product development is the verification. If the simpler model produces the same results, or similar, as the more complex models, the simpler could be used earlier in the project to gain knowledge where it is most needed. The model developed during this project has been verified by running on-centre tests to evaluate the magnitude of SWT for a certain SWA in comparison to more complex simulation models.

The developed steering controller manages the task of keeping the system stable while making it responsive. The steering feel has also shown to be objectively fulfilled, by providing a smooth and linear behaviour, and due to the tuning abilities, the subjective requirements normally present could also be fulfilled if necessary.

The ability to control the steering system and to provide the complex and functional steering feel comes from the controller layout. The different components have their task and the controller system as such takes care of most of the arbitration issues. The created framework can in the future be given more complex component algorithms, and in general more refined functionality, and still perform as supposed.

The layout of the controller gives the advantage of showing a block for each type of functionality. This greatly enhances the possibilities to understand its functions and mainly its objectives, which in turn increases the usage of the tool due to handling simplicity. As the controller has been equipped with numerous variables for tuning and altering the response of the system, the flexibility and ability to change the system is kept high. If the given response is not the same as the expected or demanded response, the model can be altered to suit the needs present. If there is a new behaviour, yet to be tried, the model is suitable to use as it can be altered as desired in its general behaviour.

The conclusion that can be drawn from this is that not only does the mechanical layout of the steering system matter, but also the controller functions. The system cannot be treated as either a rack and pinion or a passive EPAS system. The inertia and its compensation gives a too high alteration to the system. It raises the question on how to proceed with the analysis of similar types of fundamentally mechanical systems that retain controller functions modifying its response.

7 Future development and opportunities

After the project has finished, there are certain areas where development could have proceeded successfully if there had been more time available. No matter how ambitious the project is, there will always be these unfinished studies or tasks. In this section, the obvious opportunities for the future are presented.

The controller for the steering system has only been developed lightly in comparison to what is possible. There are endless possibilities to investigate for usage as improvements for the performance of the steering system. For instance, the hysteresis function can be utilized in a better way, allowing the steady state operation to be more consistent. At this point, it produces a fluctuating behaviour that is unwanted in certain situations. Another area of improvement is the active return function as it is not operating as desired at this stage. It does not always take the steering back to zero steering wheel angle after the driver lets go of the steering wheel. Another opportunity is the implementation of the feedforward controller block as it has not been used throughout the project due to lack of consistency. Finally, the active damping function could be improved with a more dynamic behaviour. With some effort, the active damping can be improved to have a more progressive behaviour to better handle instability while maintaining steering feel.

The servo motor for the model is modelled as a DC motor due to simplicity in modelling and operation. It gives a good representation of the dynamics and power draw levels in the system but a more complex model, for instance utilizing a three-phase motor, could give more accurate or useful results on assist limitations. Coupling the steering model to a battery and the rest of the vehicle electric system, would give a clearer image of the operational envelope of the steering system.

The input for the model is the steering wheel torque, which is reasonable and the best way to emulate the real steering system. However, in simulations, the input often is the steering wheel angle as it is coupled to the path of the vehicle which the torque is not. This requires a controller, or driver model, to achieve the correct steering wheel angle by supplying the correct torque. A possibility is to implement another degree of freedom that is connected to the torsion bar with a spring and damper interface. This mass could then be designed to operate as an input port for either the torque on the steering wheel or the angle of it. The steering column inertia could be divided in two so that half of the inertia was in this new mass and half could be below, effectively simulating the steering column stiffness, and a split-up inertia, that has been disregarded in this project.

A task that has been regarded as desired but not required in the project is co-simulation of the model in Adams/Car. The VI-CarRealTime model is based on data from Adams/Car but it does not capture all nonlinearities whereas Adams/Car is more accurate. To achieve full model usage, this simulation integration would be desirable and it is a task that awaits completion in the future. However, the model has been simulated together with VI-CarRealTime, meaning that the interface procedure would be comparatively straight forward for Adams/Car as well.

The steering model is more realistic than the normal steering ratio simplifications and this characteristic, together with the computational efficiency of the model, makes it suitable for driving simulator integration. Given the ability to tune the controller in a desired manor, an implementation into a simulator gives the opportunity to work with steering feel virtually using subjective assessments. The automotive industry strive towards a higher level of virtual development and the developed model supports these targets.

Further, the heavily adaptable steering system developed shows differences in behaviour, when altering the controller operation, that are significantly different. The differences are in the magnitude as of mechanical changes in the system, meaning that the controller affects the character of the model greatly. Therefore, studies on how the controller can influence and alter the system behaviour are necessary to conduct continuously.

8 Acknowledgements

The project has been executed at China Euro Vehicle Technologies AB (CEVT). The support of the company as well as its affiliates are greatly acknowledged.

The Vehicle Dynamics group in the division of Vehicle Engineering and Autonomous Systems has also been co-hosting the project and given its support which is also acknowledged.

Special thanks go to the examiner and supervisor, Mathias Lidberg, as well as to Jan Hellberg, supervisor. Jens Larsen who has been involved due to the project scope has proved to be helpful, adding an unofficial supervisor. The supervisor Ingemar Johansson has not only been helping through the project but also provided the project in the first place which requires an extra level of gratitude.

9 References

Abe, M. (2015). *Vehicle Handling Dynamics.* Elsevier Ltd.

Chugh, T., Chen, W., Klomp, M., Ran, S., & Lidberg, M. R. (2017). Design and control of model based steering feel reference in an electric power assisted steering system. Gothenburg: Chalmers University of Technology.

Fernie, M. (2018, May 24). *How Electric Power Assisted Steering Works, And Why It's Better Than Hydraulic.* Retrieved from CarThrottle: https://www.carthrottle.com/post/electronic-power-assisted-steering-how-does-it-work/

Gruner, S., Gaedke, A., Hsu, H., & Harrer, M. (n.d.). *The new EPSapa in the Porsche 911 - innovative control concept for a sports car typical steering feel.*

Harrer, M., & Pfeffer, P. (2017). *Steering Handbook.* Springer International Publishing.

Jacobson, B. e. (2016). *Vehicle Dynamics Compendium for Course MMF062.* Göteborg, Sweden: Chalmers University of Technology.

Ljungberg, M. (2014). *Electric power assist steering system parameterization and optimization employing CAE.* Stockholm: Royal Institue of Technology.

Petersson, H. (2018, April 5). Tuning of EPAS systems. (A. Gröndahl, Interviewer)

Pfeffer, P. E., Harrer, M., & Johnston, D. N. (2008). Interaction of vehicle and steering system regarding on-centre handling. *Vehicle System Dynamics*, 413-428.

Raksincharoensak, P., Lertsilpachalern, V., Lidberg, M. R., & Henze, R. (2017). Robust Vehicle Handling Dynamics of Light-Weight Vehicles Against. *Internation Conference on Vehicular Electronics and Safety* (pp. 202-207). IEEE.

Sakai, H. (2014). Design for Vehicle Stability under Force Control. *12th International Symposium on Advanced Vehicle Control.*

Smith, S. (2018, May 24). *REVIEW: PORSCHE 2012 911 CARRERA S.* Retrieved from Wired: https://www.wired.com/2012/01/porsche-911/

Uselmann, A., Kruger, K. M., Bittner, C., & Rivera, G. (2015). Innovative software functions to operate electric power steering systems in sports cars - Unterstutzungskraftregelung (UKR). *6th International Munich Chassis Symposium* (pp. 422-441). Munich: Springer.

Wallnäs, O. (2015). *Reducing the Tuning Effort of a Steer-Torque-Manager for Vehicle Lateral Control.* Stockholm: KTH Industrial Engineering and Management.

Van Ende, K. T., Kucukay, F., Henze, R., Kallmeyer, F. K., & Hoffmann, J. (2015). VEHICLE AND STEERING SYSTEM DYNAMICS IN THE CONTEXT. *International Journal of Automotive Technology*, Vol. 16, No. 5, pp. 751−763.

Van Ende, K., Kallmeyer, F., Nippold, C., Henze, R., & Kucukay, F. (2016). Analysis of steering system elasticities and their. *International Journal on Vehicle Design*, Vol. 70, No. 3.

Åström, K. J., & Wittenmark, B. (1996). *Computer Controlled Systems: Theory and Design, Third Edition.* Prentice Hall.